CellPress
PARTNER JOURNAL

Molecular Plant
Research Article

Enhanced Vitamin C Production Mediated by an ABA-Induced PTP-like Nucleotidase Improves Plant Drought Tolerance in *Arabidopsis* and Maize

Hui Zhang[1,4], Yanli Xiang[1,4], Neng He[1], Xiangguo Liu[2], Hongbo Liu[1], Liping Fang[1], Fei Zhang[1], Xiaopeng Sun[1], Delin Zhang[1], Xingwang Li[1], William Terzaghi[3], Jianbing Yan[1] and Mingqiu Dai[1,*]

[1]National Key Laboratory of Crop Genetic Improvement, Huazhong Agricultural University, Wuhan 430070, China

[2]Jilin Provincial Key Laboratory of Agricultural Biotechnology, Agro-Biotechnology Institute, Jilin Academy of Agricultural Sciences, Changchun 130124, China

[3]Department of Biology, Wilkes University, Wilkes-Barre, PA 18766, USA

[4]These authors contributed equally to this article.

***Correspondence: Mingqiu Dai (mingqiudai@mail.hzau.edu.cn)**

https://doi.org/10.1016/j.molp.2020.02.005

ABSTRACT

Abscisic acid (ABA) is a key phytohormone that mediates environmental stress responses. Vitamin C, or L-ascorbic acid (AsA), is the most abundant antioxidant protecting against stress damage in plants. How the ABA and AsA signaling pathways interact in stress responses remains elusive. In this study, we characterized the role of a previously unidentified gene, *PTPN* (*PTP-like Nucleotidase*) in plant drought tolerance. In *Arabidopsis*, (*AtPTPN* was expressed in multiple tissues and upregulated by ABA and drought treatments. Loss-of-function mutants of *AtPTPN* were hyposensitive to ABA but hypersensitive to drought stresses, whereas plants with enhanced expression of *AtPTPN* showed opposite phenotypes to . Overexpression of maize *PTPN* (*ZmPTPN*) promoted, while knockdown of *ZmPTPN* inhibited plant drought tolerance, indicating conserved and positive roles of *PTPN* in plant drought tolerance. We found that both AtPTPN and ZmPTPN release Pi by hydrolyzing GDP/GMP/dGMP/IMP/dIMP, and that AtPTPN positively regulated AsA production via endogenous Pi content control. Consistently, overexpression of *VTC2*, the rate-limiting synthetic enzyme in AsA biosynthesis, promoted AsA production and plant drought tolerance, and these effects were largely dependent on AtPTPN activity. Furthermore, we demonstrated that the heat shock transcription factor HSFA6a directly binds the *AtPTPN* promoter and activates *AtPTPN* expression. Genetic analyses showed that *AtPTPN* is required for *HSFA6a* to regulate ABA and drought responses. Taken together, our data indicate that PTPN-mediated crosstalk between the ABA signaling and AsA biosynthesis pathways positively controls plant drought tolerance.

Key words: nucleotidase, abscisic acid, vitamin C, drought, *Arabidopsis*, maize

Zhang H., Xiang Y., He N., Liu X., Liu H., Fang L., Zhang F., Sun X., Zhang D., Li X., Terzaghi W., Yan J., and Dai M. (2020). Enhanced Vitamin C Production Mediated by an ABA-Induced PTP-like Nucleotidase Improves Plant Drought Tolerance in *Arabidopsis* and Maize. Mol. Plant. **13**, 760–776.

INTRODUCTION

Higher plants are sessile organisms, which suffer from various kinds of stresses throughout their lives. Drought is one of the major abiotic stresses that negatively affect plant growth and development; therefore, higher plants have evolved sophisticated mechanisms to respond to drought. The phytohormone abscisic acid (ABA) is important for plant drought responses. During drought stress, plants increase the production of ABA, which functions as a signal resulting in the closure of stomatal guard cells to prevent water loss (Himmelbach et al., 2003). Recently, a number of regulators mediating ABA signaling have been identified. Two different groups have reported that PYL/RCAR proteins are ABA receptors (Ma et al., 2009; Park et al., 2009). Clade A PP2C phosphatases and SnRK2 kinases have also been shown to be important in ABA signaling (Raghavendra et al., 2010). A number of studies have revealed the critical roles of PYL/RCAR ABA receptors, clade A PP2C

Published by the Molecular Plant Shanghai Editorial Office in association with Cell Press, an imprint of Elsevier Inc., on behalf of CSPB and IPPE, CAS.

phosphatases, and SnRK2 kinases in the regulation of plant drought responses (Fujii and Zhu, 2009; Zhao et al., 2016; Xiang et al., 2017; He et al., 2018). The ABF/AREB (abscisic acid-responsive element binding factor) transcription factors (TFs) are downstream regulators of ABA signaling. Under drought stress, ABFs are phosphorylated and activated by SnRK2 kinases, and in turn regulate gene expression and drought responses (Yoshida et al., 2010; Fujita et al., 2013).

Another family of TFs involved in environmental stress responses are heat shock factors (HSFs) (von Koskull-Döring et al., 2007; Ohama et al., 2017). Twenty-one HSF TFs have been identified in the *Arabidopsis* genome and have been placed in three major classes (A–C) (Nover et al., 2001). A genome-wide survey of HsfA1a binding sites has been conducted. In addition to the perfect heat shock element (nTTCnnGAAnnTTCn), three novel types of binding sites have been found: gap-type, TTC-rich, and stress response element (STRE) (Guo et al., 2008), suggesting extensive roles of HsfA TFs in the regulation of gene expression. The HsfA TFs play critical roles in plant drought tolerance. Tomato HsfA1 positively regulates plant drought tolerance by activating autophagy-related (ATG) genes and inducing autophagy (Wang et al., 2015). Overexpression of *HsfA6a* in *Arabidopsis* promoted ABA sensitivity and enhanced drought tolerance, suggesting a positive role of HsfA6a in drought response (Hwang et al., 2014). Three ABA response elements (ABRE) were identified in the promoter region of *HsfA6a*. Multiple experiments demonstrated that ABF TFs, such as ABF2, ABF3, and ABF4, bind these ABREs, indicating that HsfA6a functions in drought responses via an ABA-dependent signaling pathway (Hwang et al., 2014). However, the downstream targets of HsfA6a in plant drought response remain elusive.

Drought promotes the production of reactive oxygen species (ROS), such as H_2O_2, singlet oxygen, and superoxide anion radical (O^{2-}), which cause oxidative signaling (Choudhury et al., 2017). Beyond basal levels, ROS cause oxidative stress and are toxic to cells (Mittler, 2017). Vitamin C, or L-ascorbic acid (AsA), is the most abundant of the antioxidants in plants that protect cells against oxidative stress caused by ROS (Gallie, 2013; Akram et al., 2017). In plants, AsA is mainly synthesized via the Smirnoff-Wheeler pathway, initiating from D-mannose-1-P and comprising the sequential conversion of GDP-D-mannose into GDP-L-galactose, L-galactose-1-P, L-galactose, L-galactono-1,4-lactone, and L-ascorbate (Wheeler et al., 1998; Valpuesta and Botella, 2004). Several key enzymes have been identified that catalyze the biosynthetic steps in the Smirnoff-Wheeler pathway, such as VTC1, GDP-D-mannose-3,5-epimerase (GME), VTC2, VTC4, and VTC5 (Wheeler et al., 1998; Conklin et al., 1999, 2000, 2006; Dowdle et al., 2007). VTC2 has been identified as a rate-limiting enzyme in AsA biosynthesis (Yoshimura et al., 2014). The homologs of all these Smirnoff-Wheeler pathway enzymes have been found in other plants, such as tomato, acerola, kiwifruit, and even in algal species (Badejo et al., 2009; Bulley et al., 2009; Ioannidi et al., 2009; Urzica et al., 2012), indicating that the AsA biosynthetic pathway is conserved in plants. It has been revealed that VTC2 and VTC5 are highly specific for and dependent on phosphate (Pi) for conversion of GDP-L-galactose into L-galactose-1-P (Linster et al., 2007). Although the enzymes catalyzing AsA biosynthesis have been widely studied, knowledge about the regulation of AsA production in response to environmental stresses is limited.

In this study, we characterized a previously unidentified gene, *PTPN* (for *PTP-like Nucleotidase*). Mutation of *AtPTPN* by T-DNA insertion and CRISPR editing decreased plant sensitivity to ABA but increased sensitivity to drought and osmotic stresses. In contrast, plants with enhanced expression of *AtPTPN* were more sensitive to ABA but more tolerant to drought. Overexpression of maize *PTPN* (*ZmPTPN*) enhanced and knockdown of *ZmPTPN* decreased plant drought tolerance. These observations indicated positive and conserved roles of PTPN in drought responses of *Arabidopsis* and maize. *PTPN* encodes an enzyme with nucleotidase activity that is required to regulate AsA biosynthesis. We show that *AtPTPN* expression is upregulated by drought and ABA treatments, and that HsfA6a directly binds the *AtPTPN* promoter and activates the expression of *AtPTPN*. Our findings suggest that AtPTPN could be a nexus in the ABA signaling and AsA biosynthesis pathways that positively regulate plant drought tolerance.

RESULTS

Loss-of-Function Mutants of *AtPTPN* Are Hyposensitive to ABA

ABA promotes the closure of stomatal guard cells and prevents water loss under drought (Himmelbach et al., 2003), and is therefore important for plant drought responses. Protein phosphorylation, which is regulated by protein phosphatases and kinases, has been revealed to be important for ABA signaling (Fujita et al., 2013). We screened the ABA sensitivities of ~140 T-DNA insertion mutants of genes encoding *Arabidopsis* phosphatases with unknown functions. Of these mutants, SALK_023939 was chosen for further analysis based on its ABA-response phenotypes. In the SALK_023939 mutant, the T-DNA was inserted into the 11th exon of AT3G62010 resulting in a knockout mutation (*Atptpn-1*) (Supplemental Figure 1A–1C). We further generated a knockout mutant allele of AT3G62010 (*Atptpn-2*) using the CRISPR/Cas9 system, which had a deletion of 101 bp in the first exon of AT3G62010 (Supplemental Figure 1D and 1E). The genomic sequence of AT3G62010 has 19 exons. The open reading frame (3762 nt) encodes a protein of 1254 amino acids. According to the National Center for Biotechnology Information (NCBI) protein database, AT3G62010 encodes a PTP-like phosphatase; therefore, we named this gene *AtPTPN* (*PTP-like Phosphatase*). A protein BLAST search of the NCBI protein database identified PTPN homologs in higher plants, including dicots and monocots, and even in fungi (*Schizophyllum commune*) (Supplemental Figure 2). In higher plants, the sequence identities of PTPN homologs ranged from 88% (monocots) to ~94% (dicots). The full-length AtPTPN protein apparently has three repeated regions (PTPNa–c), with 46%, 34%, and 30% identities between a/b, a/c, and b/c, respectively (Supplemental Figure 3A). This feature is conserved in all PTPN homologs across various species (Supplemental Figure 3B). Together, these data suggested evolutionary conservation of PTPN.

When grown on MS plates with ABA at various concentrations, the proportions of *Atptpn-1* and *Atptpn-2* mutants with green cotyledons were significantly higher than those of wild type

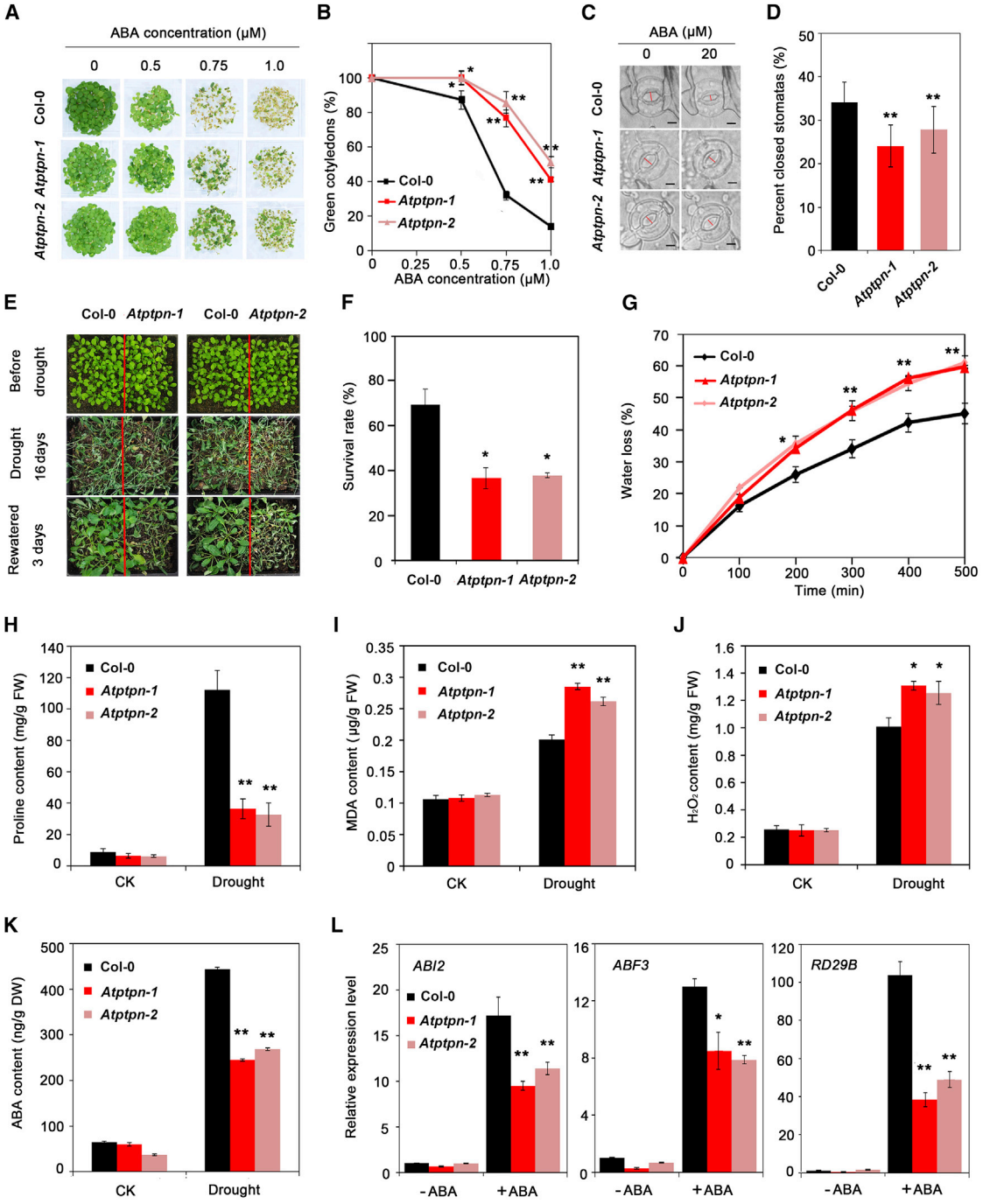

Figure 1. ABA Hyposensitivity and Drought Hypersensitivity of *Atptpn* Mutants.

(A and B) The cotyledon phenotypes **(A)** and the percentages of green cotyledons **(B)** of wild-type, *Atptpn-1*, and *Atptpn-2* plants grown in the presence of various concentrations of ABA. Col-0, *Atptpn-1,* and *Atptpn-2* seedlings were grown on MS plates with 0, 0.5, 0.75, or 1.0 μM ABA for 5 days. Data in **(B)** represent means ± SD ($n > 150$) from three biological replicates in.

(C and D) Comparison **(C)** and statistical quantification **(D)** of ABA-induced stomatal closure in Col-0, *Atptpn-1,* and *Atptpn-2* plants treated with 0, 5, 10, or 20 μM ABA. Red lines in **(C)** indicate the widest parts of the stomata. Bar, 3 μm in **(C)**. Values in **(D)** represent means ± SD ($n > 20$) from three biological replicates in.

(E and F) Drought-tolerant phenotypes **(E)** and survival rates **(F)** of soil-grown *Atptpn-1* and *Atptpn-2* mutants. Three-week-old plants were dehydrated for 16 days and then rehydrated for 3 days before phenotyping. Values in **(F)** represent means ± SD obtained from three replicates with 30 plants per replicate.

(G) Water loss rates of leaves detached from Col-0, *Atptpn-1,* and *Atptpn-2* plants. Means and SD of water loss rates were obtained from three replicates.

(legend continued on next page)

(Figure 1A and 1B). We also measured the stomatal apertures of 10-day-old wild-type, *Atptpn-1,* and *Atptpn-2* leaves in response to ABA, and observed that stomata of *Atptpn-1* and *Atptpn-2* mutants closed more slowly than those of wild type under ABA treatment (Figure 1C and 1D). Taken together, these data indicate that *AtPTPN* is a negative regulator of ABA responses.

PTPN Mutants Are Sensitive and Plants with Enhanced *PTPN* Expression Are Tolerant to Drought

The ABA hyposensitivity of stomatal closure in *AtPTPN* mutants implied that *AtPTPN* may have roles in plant drought responses. To test this hypothesis, we stopped irrigation of 4-week-old wild-type, *Atptpn-1,* and *Atptpn-2* mutant plants for ~16 days and then rewatered them. Plant survival rates were scored 3 days after rewatering. We observed significantly lower survival rates for *Atptpn-1* and *Atptpn-2* mutants (~38% on average) compared with wild type (~70% on average) (Figure 1E and 1F). In addition, detached *Atptpn-1* and *Atptpn-2* leaves lost water much faster than wild-type leaves (Figure 1G). These results indicated that *Atptpn-1* and *Atptpn-2* mutants were more sensitive to drought stress. We also observed that *Atptpn-1* mutants were more sensitive to mannitol treatment, which causes osmotic stress (Supplemental Figure 4). Proline is an osmolyte that protects plants from drought stress (Yoshiba et al., 1997). Drought-induced ROS accumulation promotes increased production of malondialdehyde (MDA). MDA is a product of lipid peroxidation, and its level is widely used as an indicator of oxidative damage to differentiate sensitivity or tolerance of plants to stresses (Hernández et al., 2000; Shalata et al., 2001; Yu et al., 2017). We investigated the production of proline and MDA in wild-type plants and *Atptpn-1* and *Atptpn-2* mutants grown under drought and well-watered conditions. The results showed that the *Atptpn-1* and *Atptpn-2* mutants produced less proline but more MDA than wild-type plants after drought stress; under well-watered conditions, there were no differences in production of proline or MDA in wild-type, *Atptpn-1,* and *Atptpn-2* plants (Figure 1H and 1I). In addition, *Atptpn-1* and *Atptpn-2* mutants produced more H_2O_2 than wild-type plants after drought stress (Figure 1J).

ABA is a key stress hormone and important for plant drought tolerance. We investigated the ABA contents in wild-type, *Atptpn-1*, and *Atptpn-2* plants. The results showed that drought promoted the production of ABA in all plants, but the increas in ABA levels in both *Atptpn-1* and *Atptpn-2* mutant plants was significantly lower than that in wild-type plants after drought stress (Figure 1K). In addition, the induced expression levels of ABA-responsive genes (*ABI2*, *ABF3,* and *RD29B*) in *Atptpn-1* and *Atptpn-2* mutant plants were lower than those in Col-0 plants after ABA treatment (Figure 1L). These results indicate reduced ABA production in *Atptpn-1* and *Atptpn-2* mutants after drought stress and impaired ABA signaling in these mutants.

Next, we expressed *AtPTPN* (35S::*AtPTPN-3HA*) in *Atptpn-1* mutants using transgenic approaches and observed that the ABA and drought phenotypes of *Atptpn-1* mutants were rescued by introduction of the transgene (Supplemental Figure 5). We also expressed 35S::*AtPTPN-3HA* in the Col-0 wild-type background to generate *AtPTPN*-overexpressing transgenic plants (OE-5, OE-6; Supplemental Figure 6A and 6B). When grown on MS plates with ABA at various concentrations, the proportions of OE-5 and OE-6 plants with green cotyledons were significantly lower than those of Col-0 (Supplemental Figure 6C and 6D). We stopped irrigation of 4-week-old soil-grown wild-type, OE-5, and OE-6 plants and then rewatered them when they showed severe stress symptoms. Survival rates were scored 3 days after rewatering. We observed significantly higher survival rates for OE-5 and OE-6 plants (~80% on average) compared with wild type (~20% on average) (Supplemental Figure 6E and 6F). After drought stress, OE-5 and OE-6 plants produced more proline, but less MDA and H_2O_2 than wild-type plants; under well-watered conditions, there were no differences in the production of these molecules in wild-type and transgenic plants (Supplemnetal Figure 6G–6I). Together, these observations suggest that *AtPTPN* plays positive roles in plant drought tolerance, perhaps by reducing the oxidation damage caused by drought.

Maize is an important crop worldwide. There is one gene, GRMZM2G146819, that encodes a maize AtPTPN homolog, ZmPTPN (Supplemental Figure 2). We overexpressed *ZmPTPN* in maize and observed that plants overexpressing *ZmPTPN* were more tolerant to drought, as revealed by higher survival rates of the positive transgenic maize plants after drought stress compared with those of their nontransgenic siblings (Supplemental Figure 7). In contrast, *ZmPTPN* knockdown plants were more sensitive to drought (Supplemental Figure 8). These studies indicate a positive and conserved role of *PTPN* in regulation of plant drought tolerance.

Temporal/Spatial and Stress-Responsive Expression of *AtPTPN*

In order to determine the temporal and spatial expression patterns of *AtPTPN*, we generated transgenic *Arabidopsis* plants harboring the *AtPTPNp*::*GUS* transgene. GUS staining assays were performed, and GUS signals were detected in roots, cotyledons, hypocotyls, guard cells, and floral organs, such as the ovule, filaments, pistils, and pollen, indicating the expression of *AtPTPN* in these tissues (Figure 2A). The expression of *AtPTPN* in multiple tissues suggested possible roles of this gene in plant development.

To determine how *AtPTPN* responds to ABA and drought treatments, 2-week-old wild-type seedlings were subjected to exogenous ABA and drought treatments, then the roots and shoots were harvested separately after various times of treatment. RT–qPCR analyses showed that in both roots and shoots, ABA strongly promoted the expression of *AtPTPN*. An increase in *AtPTPN* expression was detected after 1 h of ABA treatment,

(H–J) The contents of proline **(H)**, MDA **(I)**, and H_2O_2 **(J)** in Col-0, *Atptpn-1,* and *Atptpn-2* plants grown with or without drought stress. Values represent means ± SD (n = 3) from three biological replicates.
(K and L) ABA contents **(K)** and the expression levels of ABA responsive genes **(L)** in Col-0, *Atptpn-1,* and *Atptpn-2* plants grown with or without drought stress **(K)** or 100 μM ABA treatment **(L)**.
Statistical significance was determined by Student's t test: $^*P < 0.05$ and $^{**}P < 0.01$.

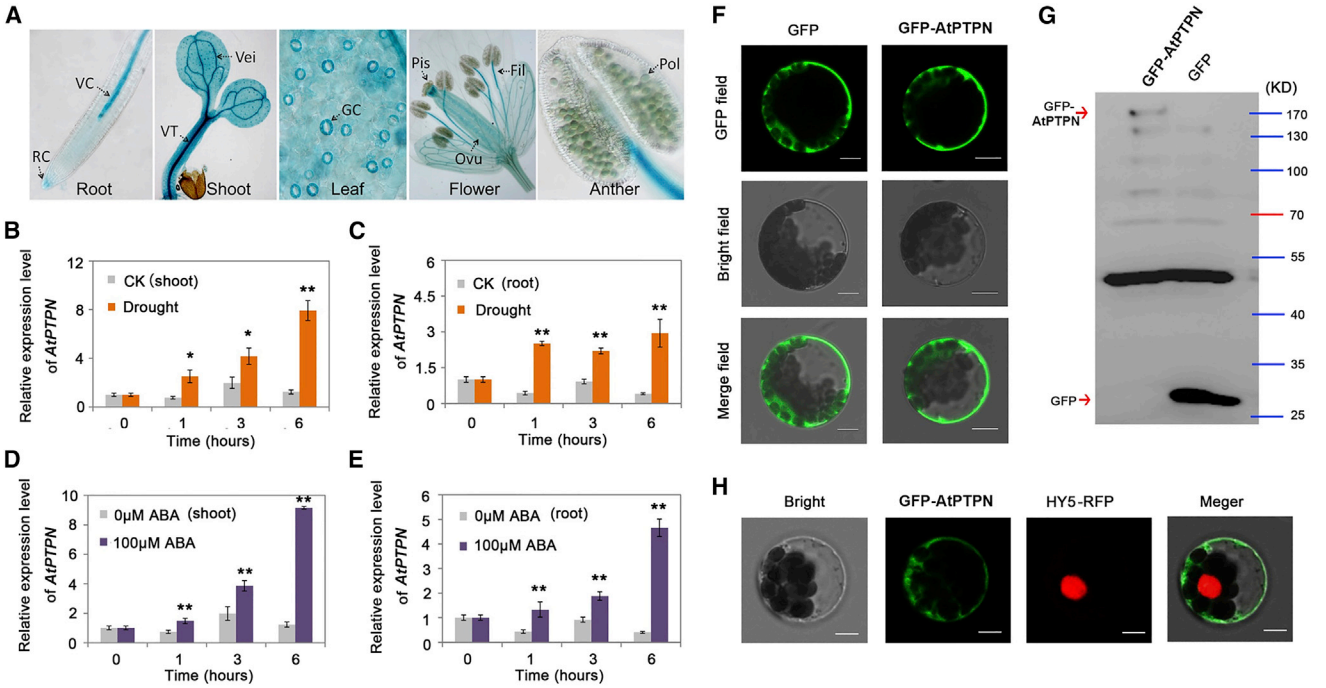

Figure 2. The Expression Patterns of *AtPTPN* and Subcellular Localization of AtPTPN.

(A) Histochemical analysis of *AtPTPN*::*GUS* activity in different tissues. Panels show the GUS activities in roots, shoots, leaves, guard cells, flowers, and anthers. All GUS staining patterns were obtained by observing at least 10 independent transgenic plants and typical pictures are shown. RC, root cap; VC, vascular cylinder; VT, vascular tissue; Vei, Vein; GC, guard cells; Pis, pistil; Fil, filament; Ovu, ovule; Pol, pollen.

(B and C) Time-course expression of *AtPTPN* in shoots **(B)** and roots **(C)** treated with or without 100 μM ABA. Values represent means ± SD (n = 3) from three replicates.

(D and E) Time-course expression of *AtPTPN* in shoots **(D)** and roots **(E)** in the presence or absence of drought stress. CK, normal growth conditions (without drought). Values represent means ± SD (n = 3) from three replicates.

(F) Subcellular localization of GFP-AtPTPN in leaf mesophyll protoplasts. Bars, 20 μm.

(G) Western blot assays showing the GFP and GFP-AtPTPN protein abundance in leaf mesophyll protoplasts.

(H) Subcellular localization of GFP-AtPTPN and HY5-RFP (a nucleus marker) in leaf mesophyll protoplasts. Statistical significance in **(B)–(E)** was determined by Student's t test: $^{*}P < 0.05$ and $^{**}P < 0.01$.

and *AtPTPN* expression was higher after 3 h of ABA treatment and continued to increase following continued ABA exposure (Figure 2B and 2C). *AtPTPN* expression was also induced by drought stress, and the induction patterns were similar to those after ABA treatment (Figure 2D and 2E). SNF1-related protein kinase subfamily 2 (SnRK2s)-encoding genes, including *SnRK2.2*, *SnRK2.3,* and *OST1* (or *SnRK2.6*), are key regulators of the ABA signaling pathway and important for plant drought tolerance (Fujii and Zhu, 2009). *AtPTPN* expression was promoted by drought, but this expression pattern of in response was abolished in *ost1* (*snrk2.6*) and *snrk2.2/2/3/6* mutants (Supplemental Figure 9), indicating that the response of *AtPTPN* to drought is dependent on ABA signaling. Together, these observations suggest that *AtPTPN* functions in drought and ABA responses, which is consistent with the results of functional studies (Figures 1 and 2).

We further investigated the subcellular localization of AtPTPN by transiently expressing 35S:*GFP-AtPTPN*, 35S:*GFP* (as a control), and HY5-RFP (nucleus localized) in mesophyll protoplast cells isolated from *Arabidopsis* leaves. We observed that GFP-AtPTPN and GFP showed similar subcellular localization in the protoplasts (Figure 2F). To exclude the possibility that the localization pattern of GFP-AtPTPN was due to the degradation of AtPTPN or failure of *AtPTPN* expression, we extracted the proteins from the protoplasts and performed western blot assays. The results showed that both GFP-AtPTPN and GFP were successfully expressed in the protoplasts transformed with 35S:*GFP-AtPTPN* and 35S:*GFP*, respectively (Figure 2G). It has been reported that GFP is localized in the cytoplasm of *Arabidopsis* mesophyll protoplasts (Ding et al., 2015). Therefore, AtPTPN could also be localized in the cytoplasm but not in the nucleus (Figure 2F and 2H).

PTPN Encodes an Enzyme with Nucleotidase Activity

We next sought to identify the substrates of PTPN. Bioinformatics analyses showed that AtPTPNa and AtPTPNb contained NCxxGxxRT motifs (x is for any amino acid) (Supplemental Figure 3), which were similar to the previously identified sequence motif forming the P loop of phytase, HCxxGxxR(T/S), which is catalytically important in hydrolyzing phytic acid (Chu et al., 2004). We therefore expressed AtPTPN in insect cells and purified the target protein to assay *in vitro* phosphatase activity. Interestingly, we did not observe any phytate hydrolysis by AtPTPN (Supplemental Figure 10A), indicating that the AtPTPN NCxxGxxRT motifs do not have phytase activity. To identify its substrates, we next tested the activity of AtPTPN toward 49 chemicals in *in vitro* activity assays

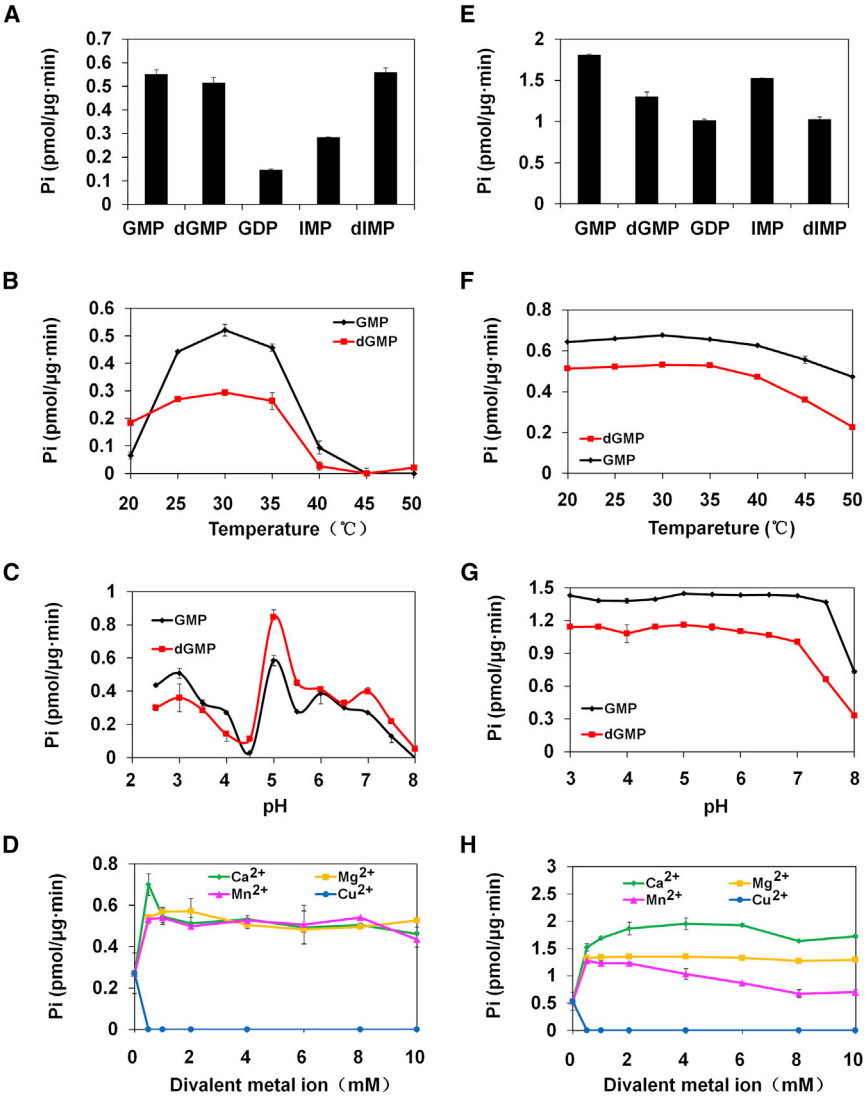

Figure 3. Enzyme Activities of AtPTPN and ZmPTPN.

(A and E) Substrate specificities of AtPTPN **(A)** and ZmPTPN **(E)** determined by enzymatic substrate screening.

(B and F) Effect of temperature on AtPTPN **(B)** and ZmPTPN **(F)** hydrolysis of GMP and dGMP.

(C and G) Effect of pH on AtPTPN **(C)** and ZmPTPN **(G)** hydrolysis of GMP and dGMP.

(D and H) Effects of different divalent metal ions on enzymatic activities of AtPTPN **(D)** and ZmPTPN **(H)**. Various divalent metal ions (Ca^{2+}, Mg^{2+}, Mn^{2+}, Cu^{2+}) at different concentrations were added to the reaction mixtures. GMP was used as the substrate for both enzymes.

Values represent means ± SD (n = 3) from three replicates for all panels.

(Supplemental Table 1). We found that AtPTPN hydrolyzed GMP, dGMP, GDP, IMP, and dIMP (Figure 3A; Supplemental Figure 10B). These results indicated that AtPTPN is an enzyme with nucleotidase activity.

Temperature, pH, and divalent metal ion concentrations are important factors affecting the activity of an enzyme. To identify the optimum temperature for AtPTPN activity, we performed activity assays with GMP and dGMP as substrates. The results showed that AtPTPN had highest activity at 30°C and was inactivated by temperatures 45°C or higher (in a range of 20°C–50°C) (Figure 3B). We next determined the pH optimum for AtPTPN using GMP and dGMP and found that at 30°C, pH 5 was optimal for AtPTPN activity toward these substrates (Figure 3C). Interestingly, another AtPTPN activity peak was observed at pH 3 while a pH of 4.5 almost inactivated AtPTPN, similar to what a pH of 8 did to this enzyme (Figure 3C). Furthermore, at 30°C and pH 5, we observed that Ca^{2+}, Mg^{2+}, and Mn^{2+} activated while Cu^{2+} killed AtPTPN activity on GMP (Figure 3D). The optimal Ca^{2+} concentration for AtPTPN activity was 0.5 mM, while there were broad concentration optima for Mg^{2+} and Mn^{2+} (0.5–10 mM) (Figure 3D). These results suggested that Ca^{2+}, Mg^{2+}, and Mn^{2+} are activators, and Cu^{2+} is an inhibitor of AtPTPN.

ZmPTPN and AtPTPN share 72% sequence identity, indicating high conservation of the PTPN sequence between maize and *Arabidopsis* (Supplemental Figure 2). To determine whether PTPN activity is conserved among plants, we performed the same substrate screening experiments for ZmPTPN. We found that ZmPTPN hydrolyzed GMP, dGMP, GDP, IMP, and dIMP (Figure 3E and Supplemental Figure 10C). Further experiments using GMP and dGMP as substrates showed that ZmPTPN had a broad temperature optimum (20°C–35°C) and pH optimum (3–7) (Figure 3F and 3G). Similar to AtPTPN, ZmPTPN was activated by Ca^{2+}, Mg^{2+}, and Mn^{2+} but inhibited by Cu^{2+} (Figure 3H). These results indicated conservation of enzyme activity between ZmPTPN and AtPTPN.

AtPTPN Activity Is Required for AsA Biosynthesis

AsA is the major plant antioxidant and protects cells by detoxification of oxidation products generated by various stresses (Gallie, 2013; Akram et al., 2017). The AsA biosynthesis pathway, the Smirnoff-Wheeler pathway, has been widely studied in plants (Wheeler et al., 1998; Valpuesta and Botella, 2004). A summary of the Smirnoff-Wheeler pathway is shown in Figure 4A. Pi has been reported to play a critical role in the conversion of GDP-L-galactose into L-galactose-1-P by VTC2 and VTC5, a rate-limiting step in AsA biosynthesis (Yoshimura et al., 2014). There is no VTC2 or VTC5 activity in the absence of Pi (Yoshimura et al., 2014). Given that AtPTPN hydrolyzed GDP/GMP/dGMP/IMP/dIMP to release Pi (Figure 3), we hypothesized that the endogenous Pi generated by AtPTPN would play a role in AsA biosynthesis. To test this hypothesis, we first investigated the AsA contents of *Atptpn-1* and wild-type plants treated with or without drought stress. The results showed that there were

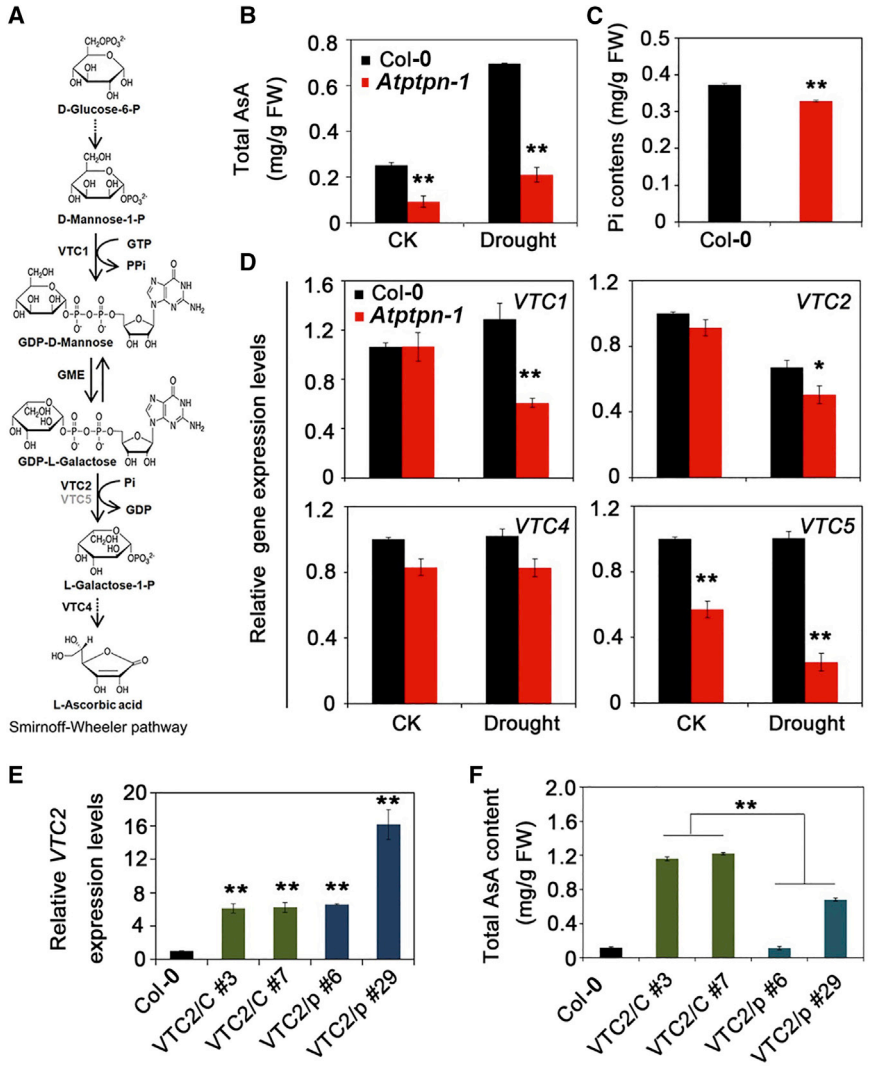

Figure 4. *AtPTPN* Regulates AsA Biosynthesis.

(A) A brief summary of the Smirnoff-Wheeler pathway. VTC1, mannose-1-P guanylyltransferase; GME, GDP mannose epimerase; VTC2/5, GDP-L-galactosephosphorylase; VTC4, L-galactose-1-phosphatase.

(B) AsA contents in 5-week-old wild-type and *Atptpn-1* mutant plants grown with or without drought stress (watering stopped for 12 days). Bars represent means ± SD of three replicates. DW, dry weight.

(C) Concentration of Pi in leaf tissues of wild-type and *Atptpn-1* mutant plants. Three-week-old seedlings were used for measurement. Error bars indicate SD (n = 3). FW, fresh weight.

(D) Expression analyses of genes encoding key AsA biosynthetic enzymes, namely *VTC1*, *VTC2*, *VTC4,* and *VTC5*, in 5-week-old wild-type and *Atptpn-1* mutant plants grown in soil with or without drought stress (watering stopped for 10 days). Bars represent means ± SD of three replicates.

(E) *VTC2* expression levels in *VTC2*/C (#3, #7) and *VTC2/p* (#6, #29) transgenic lines.

(F) AsA contents in *VTC2*/C (#3, #7) and *VTC2/p* (#6, #29) transgenic lines. Four-week-old plants were used in **(E)** and **(F)**. Bars represent means ± SD of three replicates.

(G) Drought-tolerance phenotypes and survival rates of soil-grown *VTC2*/C (#3, #7) and *VTC2/p* (#6, #29) transgenic lines. Three-week-old plants were dehydrated for 13 days and then rehydrated for 3 days before phenotyping.

Values represent means ± SD obtained from three replicates with 50 plants per replicate. Statistical significance in **(B)**–**(G)** was determined by Student's t test: $^{*}P < 0.05$ and $^{**}P < 0.01$.

reduced amounts of total AsA in *Atptpn-1* mutants compared with wild-type plants (Figure 4B). We also observed a reduction of total AsA in *Atptpn-1* mutants and wild-type plants after drought stress compared with those plants without drought stress (Figure 4B), which was consistent with the knowledge that water stress results in the depletion of the AsA pool (Smirnoff and Pallanca, 1996; Leung and Giraudat, 1998; Pastori and Foyer, 2002).

Consistent with the decreased AsA levels, the endogenous Pi content in *Atptpn-1* mutants was also significantly reduced compared with that in wild-type plants (Figure 4C). When exogenous Pi ($HPO4^{2-}$) was supplied to *Atptpn-1* mutants, we observed that AsA production recovered in these mutants (Supplemental Figure 11).

We next checked the expression of key genes in the Smirnoff-Wheeler pathway encoding the AsA biosynthetic enzymes VTC1, VTC2, VTC4, and VTC5 (Figure 5A). The results showed that the expression levels of these *VTC* genes were downregulated in *Atptpn-1* mutants compared with wild-type plants after drought stress (Figure 4D).

How VTC2, the rate-limiting enzyme in AsA biosynthesis (Yoshimura et al., 2014), regulates plant drought response remains unknown. To determine the roles of *VTC2* in drought response and how it interacts with *PTPN*, we overexpressed

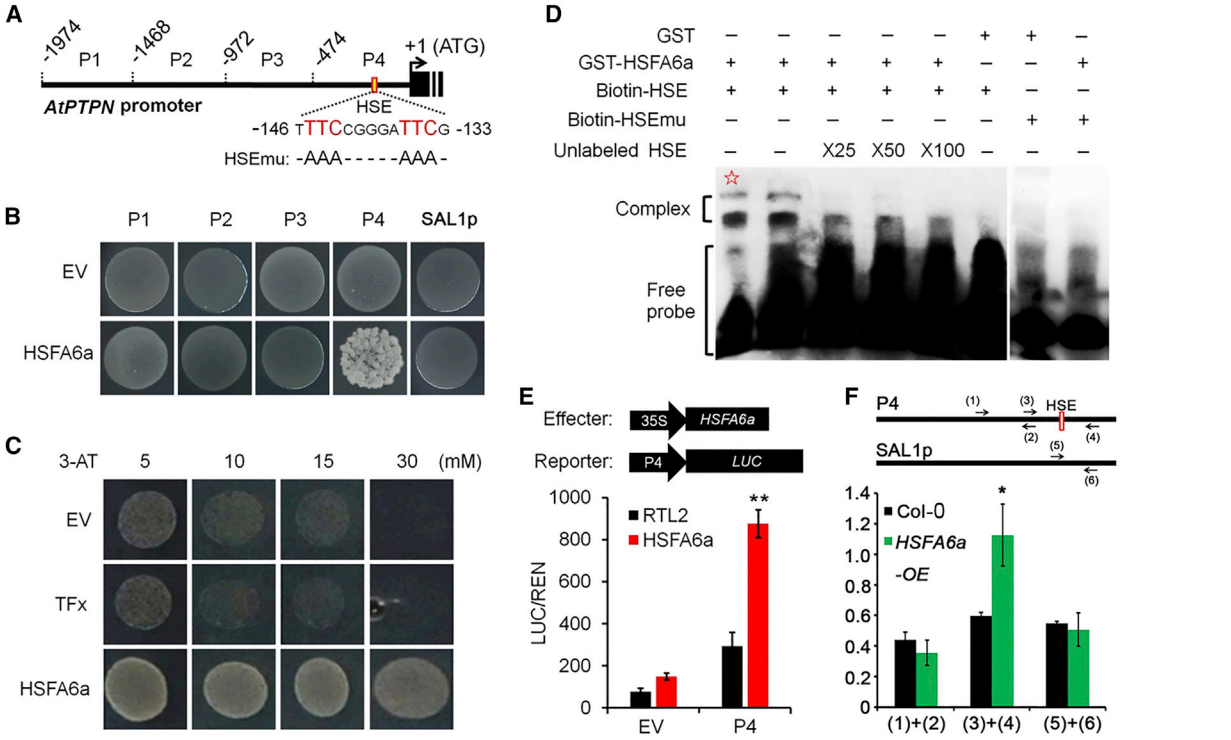

Figure 5. The Interaction between AtHSFA6a and the *AtPTPN* Promoter.

(A) A schematic diagram of the *AtPTPN* promoter region. The promoter was subdivided into four fragments designated P1, P2, P3, and P4. A heat stress element (HSE) was identified in P4 (indicated by a red box). The mutated version of this HSE is indicated as HSEmu.

(B and C) Yeast one-hybrid assays showed the interaction of HSFA6a with the P4 promoter fragment **(B)**, and 3-AT was used to suppress background growth in the experiment **(C)**. EV, empty vector. TFx, a transcription factor used as a control that shows no binding to the P4 promoter. *SAL1* promoter (SAL1p) is a negative control not bound by HSFA6a.

(D) EMSA showing HSFA6a binding to the P4 HSE motif but not the HSEmu sequence. The position of the HSFA6a–DNA complex is marked by a bracket. dI-dC was added to the reactions unless indicated with ☆ (dI-dC was not added).

(E) Luciferase assays showing the activation of expression of a P4-driven reporter by HSFA6a in Arabidopsis protoplasts. EV, empty vector. Bars represent means ± SD of three replicates.

(F) ChIP–qPCR analyses showing the binding of HSA6a to the HSE-containing DNA fragment P4 in the *AtPTPN* promoter. The primers used in qPCR after ChIP are indicated as arrows (1)–(6) on the top of the panel. *SAL1* promoter (SAL1p) is a negative control not bound by HSFA6a. Statistical significance was determined by Student's *t* test: $^{*}P < 0.05$.

this gene in wild-type (35S::*VTC2-3HA*/Col-0, or *VTC2*/C) and *Atptpn-1* mutant (35S::*VTC2-3HA*/*Atptpn-1*, or *VTC2*/*p*) plants (Figure 4E). We measured the AsA contents in the transgenic lines. The results showed that the AsA contents in *VTC2*/*p* plants were significantly lower than those in *VTC2*/C plants (Figure 4F). We also observed that the survival rates of *VTC2*/*p* plants were significantly lower than those of *VTC2*/C plants after drought stress (Figure 4G), demonstrating that VTC2 has a positive role in drought tolerance. These results also indicated that the function of VTC2 in AsA biosynthesis and drought tolerance might depend on AtPTPN activity.

HSFA6a Directly Binds the *AtPTPN* Promoter and Activates *AtPTPN* Expression

We next asked which TFs regulate *AtPTPN* expression in response to drought. To answer this question, a yeast one-hybrid screen of TFs binding the *AtPTPN* promoter was conducted using a previously reported library of 1589 *Arabidopsis* TFs (Ou et al., 2011). The promoter region of the *AtPTPN* gene (−1974 to 1) was dissected into four fragments (P1–P4) (Figure 5A), and these truncated mini promoters were expressed with the TFs in yeast cells. We found a TF, HSFA6a, that interacted with the P4 fragment in yeast cells (Figure 5B and 5C). HSFA6a is a heat shock TF classified as a member of subfamily A and plays important roles in plant drought tolerance (Hwang et al., 2014). A previous study reported that HSFA1a, another member of HSF subfamily A, binds a TTC-rich element nTTCnnnnnTTCn (n is any nucleotide) (Guo et al., 2008). Sequence analysis revealed a TTC-rich element (TTTCCGGGATTCG) in the P4 fragment (Figure 5A). To determine whether HSFA6a could bind this element (HSE, heat shock factor binding element), an electrophoretic mobility shift assay (EMSA) was performed. GST-HSFA6a bound to the biotin-labeled HSE (biotin-HSE), but not the biotin-labeled mutated HSE (biotin-HSEmu) (Figure 5A), to form complexes that migrated more slowly on the gel, and these complexes vanished after adding unlabeled HSE probes (Figure 5D). The negative control GST did not bind to biotin-HSE or biotin-HSEmu (Figure 5D). These results indicated that HSFA6a directly binds to the HSE in the P4 promoter fragment.

To ascertain whether HSFA6a could interact with the P4 fragment *in vivo*, *HSFA6a* (*35S*::*HSFA6a*) was co-expressed with the reporter *P4*::*LUC* in *Arabidopsis* protoplasts, and the relative luciferase (LUC) activity was measured. The results showed that expression of *LUC was significantly higher in protoplasts expressing* HSFA6a compared with those transformed with the empty vector pRTL2 more greatly enhanced the expression of in protoplasts (Figure 4E), implying the interaction of HSFA6a with the P4 mini promoter *in vivo*. To test whether HSFA6a binds to the HSE element of P4 in plants, we performed chromatin immunoprecipitation with quantitative PCR (ChIP–qPCR) using DNA extracted from *HSFA6a*-OE transgenic (35S::*HSFA6a-3HA*/Col-0) and Col-0 wild-type plants. Indeed, the fragment containing HSE was enriched to significantly higher levels in DNA from *HSFA6a*-OE transgenic plants compared with Col-0 DNA precipitated with HA antibody (Figure 5F). No significant difference in enrichment of a P4 fragment without an HSE, which was used as a negative control, was observed between DNA samples from *HSFA6a*-OE transgenic plants and Col-0 (Figure 5F). These results indicated that HSFA6a directly associates with the HSE in the *AtPTPN* promoter *in vivo*.

Genetic Interactions between *AtPTPN* and *HSFA6a* in ABA and Drought Responses

To learn how *AtPTPN* and *HSFA6a* genetically interact, we overexpressed *HSFA6a* in the *Atptpn-1* mutant (*35S*::*HSFA6a-3HA*/*Atptpn-1* or *HSFA 6a-OE*/p) and wild-type (*35S*::*HSFA6a-3HA*/Col-0 or *HSFA6a-OE*/C) backgrounds. Two independent transgenic lines overproducing *HSFA6a-3HA* from each background were chosen for assays (Figure 6A). In the wild-type background, overexpression of *HSFA6a* slightly enhanced the expression of *AtPTPN* (∼1.5-fold) under normal growth conditions, but more strongly (∼2.5-fold) under drought stress (Figure 6B), indicating that drought promoted the transcriptional activity of HSFA6a, and that *AtPTPN* is a target of HSFA6a activity. When treated with ABA at concentrations of 0.5, 0.75, or 1.0 μM, the cotyledons of *HSFA6a-OE*/C lines were not as green as those of wild type (Figure 6C and 6D), suggesting hypersensitivity of *HSFA6a-OE*/C lines to ABA, consistent with a previous report (Hwang et al., 2014). In the *Atptpn-1* mutant background, the ABA-hypersensitive phenotypes of *HSFA6a-OE* were rescued, and the greening ratios were higher than those of wild type (Figure 6C and 6D). In a parallel experiment, we subjected *HSFA6a-OE*/C and *HSFA6a-OE*/p transgenic plants to drought and investigated the survival rates after rewatering. The results showed that *HSFA6a-OE*/C plants were more tolerant to drought and had higher survival rates than wild type (Figure 6E and 6F), consistent with a previous report (Hwang et al., 2014). However, the *HSFA6a-OE*/p transgenic plants were more sensitive to drought and had lower survival rates than wild type (Figure 6E and 6F), indicating that mutation of *AtPTPN* affected the role of *HSFA6a* in plant drought tolerance. Taken together, these results imply that the function of *HSFA6a* in ABA and drought responses might depend on *AtPTPN* activity.

DISCUSSION

In this study, we characterized the function of *PTPN* in plant drought tolerance. We showed that loss-of-function mutants of *AtPTPN*, the *Atptpn-1* T-DNA insertion and *Atptpn-2* CRISPR mutants, were hyposensitive to ABA treatments and hypersensitive to drought. *AtPTPN* expression was detected in multiple tissues and upregulated by both ABA and drought stresses. We showed that the *PTPN* gene encodes an enzyme with nucleotidase activity. Because AtPTPN releases Pi by hydrolyzing the nucleotides GDP/GMP/dGMP/IMP/dIMP, it helps regulate AsA biosynthesis. We further demonstrated that the TF HSFA6a, whose expression is directly activated by ABF TFs in an ABA-dependent manner during drought response (Hwang et al., 2014, Supplemental Figure 12), directly binds to the HSE of the *AtPTPN* promoter, and that *HSFA6a* and *AtPTPN* function synergistically to regulate plant drought tolerance. These data together provide evidence for a working model in which drought activates the expression of *AtPTPN* via the ABF-HSFA6a pathway. AtPTPN then functions to increase the endogenous Pi content of cells to enhance AsA production and subsequently positively regulate plant drought tolerance (Figure 7).

AtPTPN Is a Novel Nucleotidase Specifically Targeting a Limited Number of Purine Nucleotides

Previous studies have revealed that FERY/SAL1 has at least two enzymatic activities in plants. It acts as a 3′(2′),5′-bisphosphate nucleotidase and an inositol polyphosphate 1-phosphatase (Quintero et al., 1996). There are various putative substrates of SAL1, including phosphoadenosine phosphosulfate (PAPS), adenosine 3′,5′-bisphosphate (PAP), and inositol polyphosphates (IPs) (Quintero et al., 1996; Xiong et al., 2004; Wilson et al., 2009; Rodríguez et al., 2010). An enzymatic motif, HCxxGxxR(T/S), is important for hydrolyzing IPs, such as inositol hexaphosphate or phytate (IP6) (Chu et al., 2004). Two similar motifs (NCxxGxxRT) were found in all PTPNs collected from various organisms in this study (Supplemental Figure 3). We thus speculated that PTPN may have phytase activity. Surprisingly, neither AtPTPN nor ZmPTPN had enzymatic activity toward IP6 (Supplemental Figure 10A). The HCxxGxxR(T/S) motif forms a P loop for binding to phytate, and the amino acid His (H) in this motif is important for P loop formation (Chu et al., 2004). There is one amino acid difference between the motif in PTPN and that in phytase (N/H). The difference in this amino acid may result in a conformational difference, resulting in different substrate preferences.

A number of chemicals were used for PTPN substrate screening in this study. Several nucleoside monophosphates and diphosphates, including IMP/dIMP, GMP/dGMP, and GDP were hydrolyzed by both AtPTPN and ZmPTPN, showing that plant PTPNs have nucleotidase activities (Figure 3, Supplemental Figure 10). Inosine monophosphate (IMP) is a precursor in the biosynthesis of purine monophosphates, such as adenosine monophosphate (AMP) and guanosine monophosphate (GMP), in both animals and plants. Xanthylate (XMP) is an intermediate in the reaction converting IMP into GMP, and thus has a molecular structure like IMP (Barsotti et al., 2005). PTPN hydrolyzed IMP and GMP, but not AMP, XMP, or other chemicals analyzed, indicating the substrate specificities of plant PTPNs. Thus far, there has been limited functional validation of plant nucleotidases. Our findings indicate that PTPN is a novel nucleotidase in plants because it specifically

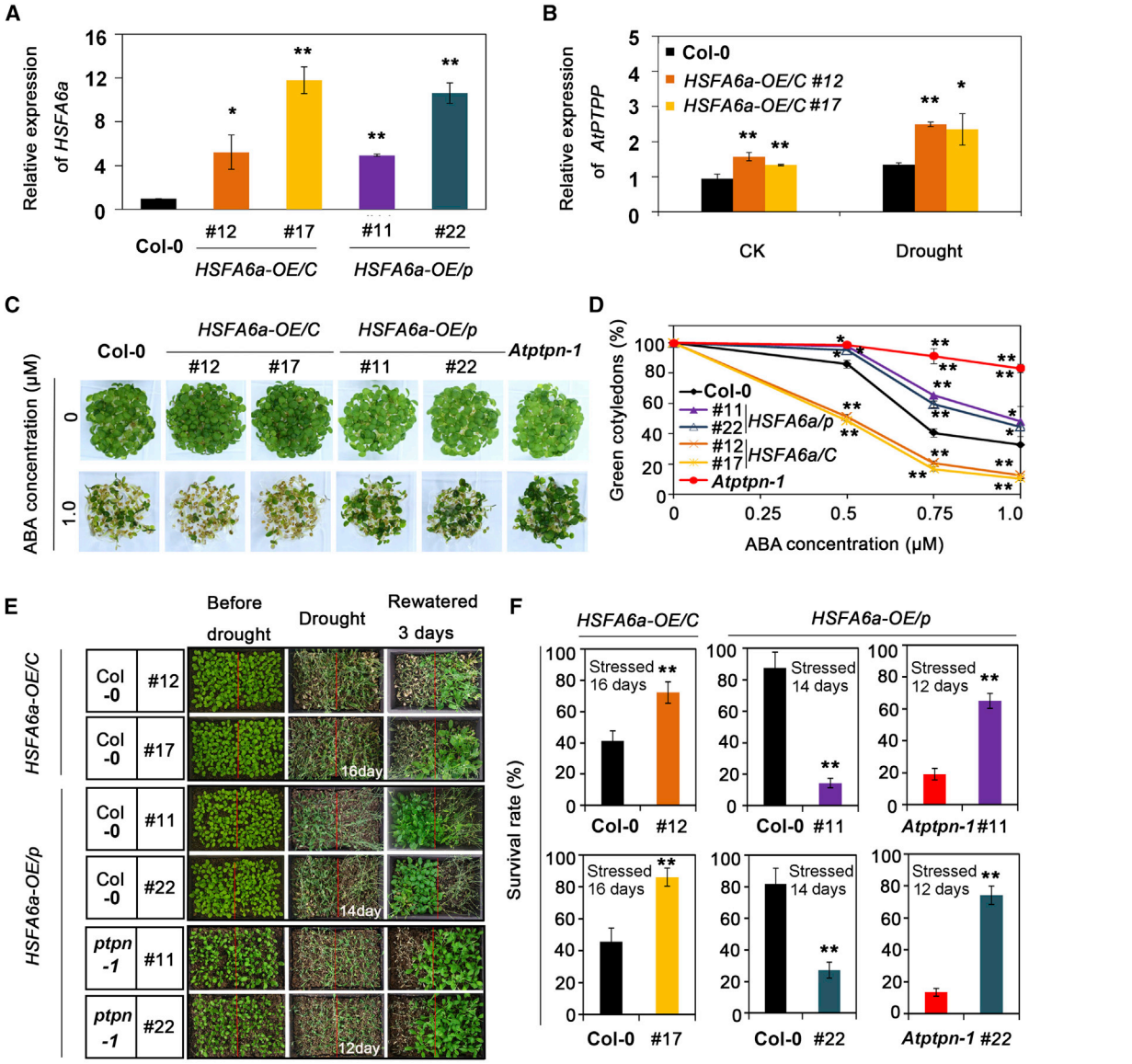

Figure 6. Genetic Interactions between *HSFA6a* and *AtPTPN* in Response to ABA and Drought Stresses.

(A) The expression levels of *HSFA6a* in Col-0, two independent *HSFA6a-OE*/Col-0 (*HSFA6a*-OE/C) lines (#12, #17), and two independent *HSFA6a-OE*/*ptpn* (*HSFA6a*-OE/p) lines (#11, #22). Two-week-old transgenic and wild-type plants were used in these expression assays. Bars are the means ± SD of three replicates.

(B) The expression levels of *AtPTPN* in Col-0 and *HSFA6a*-OE/C (#12, #17) plants in the presence or absence of drought stress. Two-week-old transgenic and wild-type plants were dehydrated on dry filter paper, and shoots were sampled at 0 and 1 h for expression assays. Bars are the means ± SD of three replicates.

(C and D) The cotyledon phenotypes **(C)** and the percentages of green cotyledons **(D)** of wild type, *HSFA6a*-OE/C (#12, #17), *HSFA6a*-OE/p (#11, #22), and *ptpn* under various concentrations of ABA. Col-0, *HSFA6a-OE/C, HSFA6a-OE/p,* and *ptpn* seedlings were grown on MS plates with 0, 0.5, 0.75, or 1.0 μM ABA for 5 days before phenotyping. Values represent means ± SD ($n > 150$) from three biological replicates.

(E and F) Drought-tolerance phenotypes **(E)** and survival rates **(F)** of wild-type, *HSFA6a-OE/C,* and *HSFA6a-OE/p* plants after drought treatment. Plants were grown in soil side by side. Three-week-old plants were dehydrated for 12, 14, or 16 days as indicated and then rehydrated for 3 days before phenotyping. Bars in **(F)** are the means ± SD ($n = 30$) of three replicates in.

Statistical significance was determined by Student's *t* test: $^{*}P < 0.05$, $^{**}P < 0.01$.

targets a limited number purine nucleotides, in contrast to SAL1, and has important roles in plant stress tolerance. The molecular mechanism by which PTPN hydrolyzes its substrates is currently unknown. In the future, it will be worth dissecting the functional amino acids or motifs of PTPN via protein crystal-structure analysis.

PTPN Is an Important Regulator of Oxidative Stress Responses

GME is an important AsA synthetic enzyme converting GDP-D-mannose into GDP-L-galactose (Wheeler et al., 1998). Overexpression of *MsGME* in *Arabidopsis* increases the AsA levels and enhances drought tolerance (Ma et al., 2014).

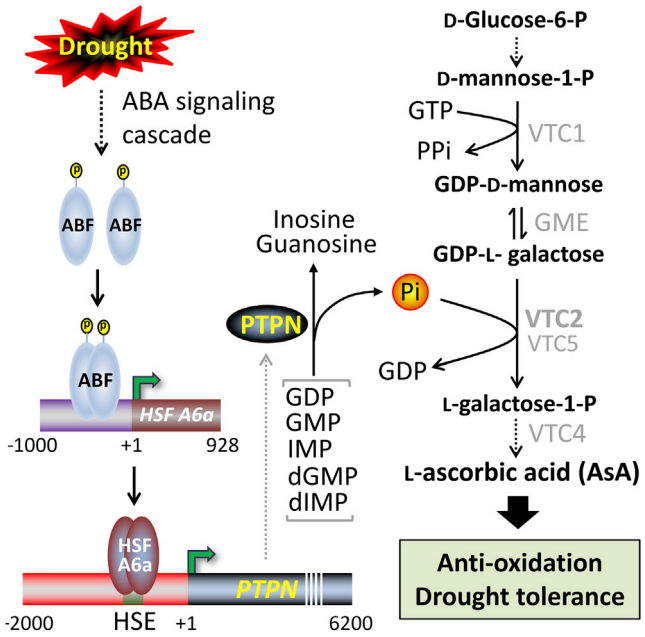

Figure 7. A Working Model for AtPTPN.

In this model, AtPTPN functions at the nexus of the ABA signaling and AsA biosynthesis pathways involved in plant drought tolerance. Drought enhances ABA signaling, which in turn leads to the phosphorylation and activation of the ABF transcription factors (TFs). The active ABF TFs promote *HSFA6a* expression by binding to the ABRE in the *HSFA6a* promoter. HSFA6a in turn enhances *AtPTPN* expression levels by binding to the HSE in the *AtPTPN* promoter. AtPTPN hydrolyzes GDP/GMP/dGMP/IMP/dIMP to increase endogenous Pi content, which enhances AsA production and facilitates plant drought tolerance.

Exogenous application of AsA enhances the drought tolerance of various plant species, including maize (Darvishan et al., 2013), wheat (Malik and Ashraf, 2012; Hussein et al., 2014), sunflower (Ahmed et al., 2013), savory (Yazdanpanah et al., 2011), okra (Amin et al., 2009), and canola (Shafiq et al., 2014). Our study also showed that overexpression of VTC2, the rate-limiting enzyme in AsA biosynthesis, greatly enhanced plant drought tolerance (Figure 4). Our data have demonstrated positive roles of PTPN in the control of AsA production via release of endogenous Pi in response to drought. *Atptpn-1* mutants still had some AsA, indicating that plants can use Pi from multiple sources to synthesize AsA.

During drought or other abiotic stresses, and even biotic stresses, production of many ROS molecules, including H_2O_2, singlet oxygen, and superoxide anion radicals, is enhanced. These overaccumulated ROS cause oxidative stress damage to membrane lipids, DNA, RNA, and protein molecules (Mittler, 2017). AsA is the most abundant water-soluble antioxidant compound present in plant tissues and can directly scavenge ROS molecules and protect membrane systems from oxidative stress (Gallie, 2013; Akram et al., 2017). There were lower AsA levels in the *Atptpn-1* mutants compared with wild-type plants. The H_2O_2 contents and MDA levels in *Atptpn-1* mutants were significantly higher than those in wild-type plants (Figure 1). Thus, *Atptpn-1* mutants partially lost their ability to scavenge ROS molecules and reduce oxidative stress, and this may have resulted in the sensitivity of *Atptpn-1* mutants to drought. To our knowledge, PTPN is the only nucleotidase identified so far to regulate AsA production. Given that AsA is the main antioxidant in plants, our data suggest that PTPN might play important roles in multiple stress responses via anti-oxidative mechanisms.

AtPTPN Acts at the Nexus of the ABA Signaling and AsA Biosynthesis Pathways

It has been reported that the HSF TFs generally bind to the canonical *cis*-element nGAAnnTTCn (von Koskull-Döring et al., 2007). A recent study demonstrated that HSFA1a positively regulates drought tolerance by binding the canonical HSE of ATG genes and regulating their expression (Wang et al., 2015). Besides the canonical HSE, a previous study based on chromatin immunoprecipitation (ChIP) has revealed six putative novel HSFA1a binding motifs that can be classified into three groups: gap-type, TTC-rich-type, and STRE (Guo et al., 2008). There is a TTC-rich-type HSE motif (TTTCCGGGATTCG) in the *AtPTPN* promoter (Figure 4). EMSA and ChIP–qPCR assays demonstrated that HSFA6a could directly bind to this HSE motif in the *AtPTPN* promoter. Thus, the subfamily A HSF TFs could regulate the expression of downstream genes by binding various HSE motifs in response to drought.

There were reduced ABA levels in *Atptpn-1* and *Atptpn-2* mutants, and ABA signaling was impaired in these mutants (Figure 1), suggesting that *AtPTPN* might regulate drought tolerance in an ABA-dependent manner. *Arabidopsis HSFA6a* has been previously reported to play roles in plant drought responses. Our experiments indicated that drought-activated *HSFA6a* is dependent on ABA signaling (Supplemental Figure 12). Plants overexpressing *HSFA6a* have increased ABA sensitivity and drought tolerance (Figure 5; Hwang et al., 2014). ABF TFs are known to be phosphorylated and activated by ABA signaling and positively regulate plant drought tolerance (Yoshida et al., 2010; Fujita et al., 2013). The expression of *HSFA6a* is activated by ABA via binding of ABFs to the ABREs in the *HSFA6a* promoter (Hwang et al., 2014). The enhanced expression of *AtPTPN* in *HSFA6a-OE*/C plants indicated that HSFA6a activates the expression of *AtPTPN*. Binding of HSFA6a to the HSE motif of the *AtPTPN* promoter indicated that *AtPTPN* could be a direct target of HSFA6a in drought responses. In addition, the function of HSFA6a in response to ABA and drought largely depends on AtPTPN activity (Figure 5). Therefore, AtPTPN likely functions at the nexus of the ABA signaling and AsA biosynthesis pathways to control plant drought tolerance (Figure 7). Given the conserved role of *PTPN* in plant drought tolerance (Supplemental Figures 7 and 8), this gene may potentially be of use in genetic engineering for breeding of drought-tolerant crops.

METHODS

Plant Materials and Growth Conditions

Arabidopsis thaliana ecotype Col-0 was used as the wild type in this study. The T-DNA insertion mutant of *Atptpn-1* (SALK_023939) was ordered from the ABRC. The presence of the T-DNA insertion was verified by genotyping and expression assays with primers SALK_LB1.3, *Atptpn-1*-F/R, and Actin3-F/R. The *ost1*, *snrk2.2/3/6*, and *abf3/4* mutants were reported previously (Fujii and Zhu, 2009; Fujita et al., 2013). Seeds were first stratified for 3 days at 4°C in the dark after being surface-sterilized with 10% bleach

and 0.025% Triton X-100 for 10 min, washed with sterile distilled water three times, and then sown on full-strength MS plates (4.4 g/l MS powder, 10 g/l sucrose, and 8 g/l agar [pH 5.7]). Seeds were germinated and grown in a growth chamber at 22°C (light period, 16 h light/8 h dark; illumination, 5800 lux; relative humidity, 60% ± 5%). Ten-day-old seedlings were transferred into soil and grown in a culture room (light period, 16 h light/8 h dark; illumination, 8000 lux; relative humidity, 70% ± 5%; temperature, 22°C–24°C).

Bioinformatics Analysis

To explore the phylogenesis of *PTPN* genes, a BLAST search against the genomes of multiple plant species in EnemblPlants(http://plants.ensembl.org/index.html) was performed. The *Arabidopsis* PTPN sequence was used as the query in this assay. Full-length amino acid sequences of all identified PTPN genes were aligned using MUSCLE built in MEGA6 (https://www.megasoftware.net/) with default parameters. Then, a phylogenic tree was constructed in MEGA6 using the neighbor-joining (NJ) method with the following parameters: pairwise deletion, uniform rates, and 1000 bootstrap replicates. All aligned PTPN sequences were submitted to Weblogo (http://weblogo.berkeley.edu/logo.cgi) to generate the seqlogo figure.

Plant Transformation

CRISPR/Cas9-based genome editing technology was used in this study to generate *Atptpn-2* gene-edited *Arabidopsis* lines. Effective guide RNAs targeting *AtPTPN* were predicted and obtained using the web-based *CRISPR PLANT* software (http://www.genome.arizona.edu/crispr/CRISPRsearch.html) (gRNA1, GATACCGAAGGAGCCAGAGC; gRNA2, CAGATCGAAGGCGCTCCTAA). Two gRNAs targeting *AtPTPN* were cloned into a gRNA backbone by PCR with primers gRNA1-F/R and gRNA2-F/R using pCBC-DT1T2 as template, and then the *AtPTPN* gRNA backbone was inserted into the pHEE401 vector using T4 ligase; BsaI was used in the linearization of pHEE401 to produce pHEE401-*AtPTPNCrispr*. The recombinant plasmids were transformed into *Agrobacterium tumefaciens* stain GV3101. *Agrobacterium*-mediated transformation into the wild type (Col-0) was performed using the floral dip method. Positive transformants were selected on MS plates containing 25 μg/ml hygromycin. Homozygous lines were identified by amplifying and sequencing fragments surrounding the target sites of *AtPTPN* with gene-specific primers CRISPR-CX-F/R.

For overexpression of *AtPTPN*, the coding sequence (CDS) of *AtPTPN* was amplified by PCR using *Arabidopsis* cDNA as template with primers AtPTPN-F′/R′ and then inserted into pCAMBIA1305-3HA using a recombination kit (Vazyme). KpnI and XbaI were used in the linearization of pCAMBIA1305-3HA to generate pCAMBIA1305-*AtPTPN-3HA*. The recombinant plasmids were transformed into *A. tumefaciens* stain GV3101. *Agrobacterium*-mediated transformation of wild type (Col-0) and *Atptpn-1* mutants was performed by the floral dip method. Positive transformants were selected on MS plates containing 25 μg/ml hygromycin. Single copy lines were identified based on a segregation ratio of 3:1 (surviving/dead) on selective MS plates. Homozygous lines were used for further analysis.

For the GUS staining assay, a 2000 bp DNA fragment upstream of the translation start site of *AtPTPN* was cloned with primers *AtPTPNpro*-F/R and inserted into the pCAMBIA1300-*GUS* vector to drive the expression of *GUS*. The pCAMBIA1300-*AtPTPNpro*-GUS plasmid was introduced into *A. tumefaciens* strain GV3101 and transformed into the *Arabidopsis* Col-0 ecotype using the floral dip method. Positive transformants were selected on MS plates containing 50 μg/ml Basta. The homozygous lines showing stable expression of *GUS* were selected for further analysis.

For overexpression of *VTC2*, the CDS of *VTC2* was amplified by PCR using *Arabidopsis* cDNA as template with primers VTC2′-F/R and then inserted into pCAMBIA1305-3HA; KpnI and SalI were used in the linearization of pCAMBIA1305-*3HA* to generate pCAMBIA1305-*VTC2-3HA*. For overexpression of *AtHSFA6a*, *AtHSFA6a* was amplified by PCR using *Arabidopsis* genomic DNA as template with primers AtHSFA6a-F/R and then inserted into pCAMBIA1305-3HA; KpnI and XbaI were used in the linearization of pCAMBIA1305-*3HA* to generate pCAMBIA1305-*AtHSFA6a-3HA*. The recombinant plasmids were transformed into *A. tumefaciens* stain GV3101. *Agrobacterium*-mediated transformation into the wild type (Col-0) and *Atptpn-1* mutant was performed using the floral dip method. Positive transformants were selected on MS plates containing the 25 mg/ml hygromycin. Single copy lines were identified based on a ratio of 3:1 (surviving/dead) on selective MS plates. Homozygous lines were used for further analysis.

For overexpression of *ZmPTPN* in maize, the *ZmPTPN* CDS was amplified by RT-PCR using cDNA of B73 as template with primers ZmPTPN-F/R. The fragment was inserted into pZZ0153 using a recombination kit (Vazyme). XmaI and AscI were used in the linearization of pZZ0153 to produce the pZZ0153-ZmPTPN vector. For RNA interference (RNAi) of *AtPTPN*, PDKin (PDK intron) fragments were amplified by PCR using pSAT6-PDKin as template with the primers PDKin-F/R and then inserted into pZZ0153. SmaI was used in the linearization of pZZ0153 to produce the pZZ0153-PDKin vector. *ZmPTPN* RNAi fragments were amplified by PCR using DNA of B73 as template with *ZMPTPN* (RNAi)-F/R as primers and then inserted into the sites flanking the PDKin fragment in pZZ0153-PDKin using T4 ligase. SpeI and PmeI were used in the linearization of pZZ0153-PDKin to produce the pZZ0153-*ZMPTPN* (RNAi)-PDKin vector. XmaI and AscI were used in the linearization of pZZ0153-*ZMPTPN*(RNAi)-PDKin to produce the pZZ0153-*ZMPTPN* (RNAi)-PDKin-*ZMPTPN*(RNAi) vector (the two ZmPTPN [RNAi] fragments are inserted in opposite orientations). China National Seed Group Co., Ltd performed the gene transformations into the maize inbred line C01.

Abiotic Stress Treatments

For the ABA treatments, seeds were sown on MS medium plates with different concentrations of ABA (Sigma-Aldrich), and after 5–6 days, cotyledon greening was visualized under a microscope. To observe changes in root length, seeds were germinated and grown vertically on MS plates for 4 days and transferred onto fresh MS plates with different concentrations of ABA for 10 days, and then the root length was calculated using ImageJ software. For the osmotic stress tolerance test, seeds were germinated and grown vertically on MS for 4 days, transferred onto MS plates with different concentrations of mannitol for 10 days, and then the root length, shoot fresh weight. and contents of proline and anthocyanin were measured.

For qRT–PCR expression assays, seeds were germinated and grown vertically on MS plates for 2 weeks, treated with 100 μM ABA in liquid full-strength MS medium or dehydrated on dry filter paper for various periods, and then frozen in liquid nitrogen for further analyses. For the drought stress experiments, plants were grown for 3 weeks in a growth chamber with 16 h light/8 h dark, 8000 lux illumination, 70% ± 5% relative humidity, a temperature of 22°C–24°C, and∼90% soil moisture (garden soil), and subjected to drought stress by withholding water for 14 ± 2 days (the exact number of days for each treatment are shown in the figures and legends). The plants were rewatered, and surviving plants were counted 3 days after rewatering. For maize drought experiments, imbibed seeds were grown in soil in a greenhouse (approximately 30°C) under normal watering conditions (field soil with 30%–40% moisture) until the 4-leaf stage, and the plants were subjected to drought stress for 10 days. The plants were rewatered, and the surviving plants were counted 7 days after rewatering. In parallel experiments, leaves from plants were harvested after drought treatment for 10 days, and the ascorbic acid, proline, H_2O_2 and MDA contents were determined. For all the above assays, at least three independent experiments were performed.

Pi Treatment

For Pi treatment, Col-0 and *Atptpn-1* seeds were germinated and grown on MS plates for 7 days and then transferred into soil and grown at

22°C–24°C under long-day conditions (16 h light/8 h dark). Four weeks after transplanting, the plants were watered with 1 mM KH_2PO_4 (+Pi) or 1 mM KCl (CK, −Pi) every 2 days. Five days after the treatments, the rosette leaves of the plants were harvested for measurement of AsA content.

Histochemical GUS Staining

The histochemical GUS staining was performed as described in our previous report (Dai et al., 2012) with minor modifications. Briefly, tissues from *AtPTPNpro*:*GUS* transgenic plants at different developmental stages were collected and submerged in GUS staining solution (50 mM sodium phosphate [pH 7.0], 0.5% Triton X-100, 5 mM EDTA, 0.5 mM $K_3Fe(CN)_6$, 0.5 mM $K_4Fe(CN)_6$, and 2 mM 5-bromo-4-chloro-3-indolyl glucuronide) at 37°C for 16 h. To remove chlorophyll after GUS staining, the tissues were immersed in acidic acid/alcohol (6:1) and mounted with a mixture of chloral hydrate/distilled water/glycerol (8:3:0.5) before observation with a light microscope. The digital images were taken using Nikon NIS Elements D software.

RNA Purification and Expression Analysis

Total RNA was isolated from the seedlings with Trizol reagent according to the manufacturer's instructions (Thermo Scientific); 1.5 μg of total RNA was used for reverse transcription with M-MLV reverse transcriptase and oligo(dT) primers according to the manufacturer's instructions (Promega). Single-stranded cDNA was used for expression analyses. At least three biological replicates per experiment were sampled, and each sample was run in triplicate. The *Arabidopsis actin* gene was used as an internal control to normalize the data. For each primer pair, the amplification efficiency was evaluated by melting-curve analysis.

Protein Isolation and Enzymatic Assays

Protein expression and purification were performed as previously described (Wang et al., 2016). Briefly, *AtPTPN* and *ZmPTPN* were amplified by PCR using cDNA of Col-0 and B73 as templates with primers *AtPTPN*-S-F/R and ZmPTPN-C-F/R, respectively, and then *AtPTPN* fragments were inserted into a modified pFastBac1 vector with an SUMO affinity tag fused to the N terminus. *ZmPTPN* fragments were inserted into a modified pFastBac1 vector with a His affinity tag fused to the C terminus using a recombination kit (Vazyme). BamHI/XhoI and NdeI/XhoI were used in the linearization of pFastBac1-Sumo and pFastBac1-His to produce the pFastBac1-Sumo-AtPTPN and pFastBac1-ZmPTPN-His vectors, respectively. Bacmids were generated in DH10Bac cells following the instructions for the Bac-to-Bac baculovirus expression system (Invitrogen), and baculoviruses were generated and amplified in Sf-9 insect cells. For protein expression and purification, cells were harvested by centrifugation at 2000 *g* for 15 min and homogenized in ice-cold lysis buffer containing 25 mM Tris–HCl (pH 8.0), 150 mM NaCl, and 0.5 mM phenylmethanesulfonylfluoride. The cells were disrupted using a cell homogenizer. The insoluble fraction was precipitated by ultracentrifugation (20 000 *g*) for 1 h at 4°C. The supernatant was loaded onto a Ni-NTA superflow affinity column (QIAGEN) and washed three times with lysis buffer plus 10 mM imidazole. Elution was performed in buffer containing 25 mM Tris–HCl (pH 8.0) and 250 mM imidazole. The purified protein was used for enzyme activity assays.

Enzymatic assays were performed as previously described (Kuznetsova et al., 2005) with minor modifications. Briefly, for the substrate screening assay, the reactions were performed in 96-well microplates using 160 μl of reaction mixture containing 50 mM HEPES–KOH (pH 7.5), 0.25 mM substrate, and 1 μg of enzyme protein at 37°C for 20 min. Activity profiles of AtPTPN and ZmPTPN were determined at different temperatures, pHs, and concentrations of divalent metal ions. The optimum temperatures of AtPTPN and ZmPTPN were determined by incubating the assay mixture at different temperatures in the range of 20°C–70°C for 15 min in HEPES–KOH buffer (pH 7.5) with 1 μg of protein and 0.25 mM substrate. The optimum pHs of AtPTPN and ZmPTPN were determined by incubating the assay mixture in different buffers with different pHs in the range of 2.5–8.0 for 15 min with 1 μg of protein and 0.25 mM substrate. The following buffers were used for the indicated pH ranges: glycine–HCl, pH 2.5–4; Na acetate–acetic acid, pH 4.5–5.5; Tris–acetic acid, pH 6.0–6.5; HEPES–KOH, pH 7.0–8.0. The optimum divalent metal ions for AtPTPN and ZmPTPN were determined by adding 0–10 mM divalent metal ion (Ca^{2+}, Mg^{2+}, Mn^{2+}, Cu^{2+}) into the reaction mixtures (50 mM HEPES–KOH buffer [pH 7.5] with 1 μg of protein and 0.25 mM substrate) and incubating the reaction mixture at 30°C for 15 min. All reactions were terminated by addition of 40 μl of malachite green reagent, and the production of Pi was measured at 630 nm 5 min later. All reactions were done in triplicate. Results were compared with a standard curve prepared with inorganic phosphate (KH_2PO_4). The enzyme activity was defined as amount of phosphate released per minute per milligram of enzyme protein under the specified assay conditions.

Water Loss Assay

For water loss measurements, the detached leaves from 3-week-old plants were exposed to air at room temperature (~25°C) and weighed at 100-min intervals using a microbalance. Water loss rates were recorded at 500 min after dehydration and measured as a percentage of the initial weight of fully hydrated leaves.

Stomatal Aperture Assay

The stomatal aperture was measured essentially as previously described (Ding et al., 2015). Briefly, epidermal peels from rosette leaves of 3-week-old *Arabidopsis* plants were floated in stomatal opening solution (10 mM KCl, 50 μM $CaCl_2$, 10 mM MES [pH 6.15]) and exposed to light for 2–2.5 h to achieve full opening of the stomata. Subsequently, ABA was added to the opening solution to a final concentration of 0 or 10 μM and epidermal peels were incubated for 1 h to induce stomatal closure. After incubation, stomata were photographed and stomatal apertures in the presence or absence of 10 μM ABA (at least 40 stomatal apertures per treatment) were measured (width/length) using ImageJ software.

Subcellular Localization of AtPTPN

To express the GFP-AtPTPN fusion protein, the coding region of *GFP* was amplified by PCR using pSAT6-TAG as template with primers GFP-F/R, and then inserted into pRTL2. SacI and XbaI were used in the linearization of pRTL2 to generate pRTL2-*GFP*. Next, the coding region of *AtPTPN* was amplified with primers AtPTPN (C)-F/R and then inserted into the pRTL2-*GFP* vector using a recombination kit (Vazyme). BamHI and XbaI were used in the linearization of pRTL2-*GFP* to generate pRTL2-*GFP*-*AtPTPN*. The plasmids were used for protoplast transformation according to a protocol developed by Jen Sheen (http://genetics.mgh.harvard.edu/sheenweb/). After transformation, the protoplasts were incubated at 22°C in the dark for 16 h. Then, the fluorescence signals of GFP were examined with a confocal microscope (Leica).

Yeast One-Hybrid Assay

The yeast one-hybrid assay was performed using the MATCHMAKER One-Hybrid System (PT1031-1). Briefly, DNA fragments from the promoter of *AtPTPN* (P1, P2, P3, and P4) were amplified from Col-0 DNA with primers *PTPNpro*-F1/R1, *PTPNpro*-F2/R2, *PTPNpro*-F3/R3, and *PTPNpro*-F4/R4, respectively. The *AtPTPN* promoter fragments were then inserted into the pHISi-1 plasmid as bait to trap proteins that can bind to the promoter of *AtPTPN*. A library of *Arabidopsis* TFs was used in this assay. The yeast strains YM4271 and Y187 were used for bait clones and prey clones. Strains containing the various TF proteins or fragments of the *AtPTPN* promoter were mated pairwise and screened on His-Trp-dropout media. 3-AT was used to suppress background growth in this experiment.

Electrophoretic Mobility Shift Assay

The *HSFA6a* gene was cloned into the pGEX-4T vector containing an N-terminal *GST* CDS. The fusion and empty constructs were transformed

into BL21 *Escherichia coli* cells. The fusion proteins were purified according to the manufacturer's procedure. The probes were created by annealing complementary biotinylated oligonucleotides. EMSAs were performed using a LightShift Chemiluminescent EMSA kit (Thermo Scientific). Each binding reaction contained 40 fmol of biotin-labeled probe and 5 μg of protein. The unlabeled probes were used as competitors. A 5% polyacrylamide gel in 0.5× TBE was pre-run for 40 min at 4°C. Five microliters of 5× loading buffer was added to each binding reaction, and subsequently, each reaction was subjected to gel electrophoresis at 100 V for 1 h. The probes and proteins on the gel were then transferred to a charged nylon membrane (100 V, 50 min), and the membrane was UV crosslinked at 120 mJ/cm^2 for 1 min. The membrane was treated with developing buffers according to the manufacturer's protocol and then exposed to film and developed.

Luciferase Assay

The P4 fragment derived from the At*PTPN* promoter was cloned into pGL3-Basic to drive the expression of the firefly luciferase reporter. The effector *HSFA6a* was cloned into pRTL2 downstream of the 35S promoter. *Arabidopsis* leaf protoplasts were isolated from 4-week-old soil-grown plants and inoculated with various constructs according to a protocol developed by Jen Sheen's lab (http://genetics.mgh.harvard.edu/sheenweb/). After transformation, the protoplasts were incubated at 22°C for 16 h. Firefly and Renilla luciferase were quantified with a dual-luciferase reporter assay according to the manufacturer's instructions (Promega). Three independent transformation assays were used to calculate the mean and SE for luciferase expression.

ChIP Assay

ChIP assays were performed as previously described (Kaufmann et al., 2010). Briefly, 3-week-old Col-0 and *HSFA6a*-OE/Col-0 seedlings (about 2 g) were crosslinked in 1% formaldehyde for 25 min. Then the nuclei were isolated and resuspended in high-salt nuclear lysis buffer. Chromatin was sonicated to an average size of 100–500 bp using the Bioruptor (Diagenode). The protein–DNA complexes were immunoprecipitated by a mouse HA antibody (NewEast, catalog no. 28003). After elution and reverse crosslinking, the enriched DNA was purified for qPCR.

Measurement of Anthocyanin

The experiments were performed as described in a previous report (Mancinelli, 1990) with minor modifications. Briefly, 20 mg of rosette leaves from seedlings were collected and placed in 2 ml of extraction solution (1% HCl in methanol) at 4°C for 16 h. The absorbance of extracts was measured at A530 and A657. The quantity of anthocyanin was determined as A530 − 0.25 × A657.

Measurement of Malondialdehyde

Extraction was performed by homogenization of 0.2 g of leaf tissue with 2 ml of 5% (w/v) trichloroacetic acid and centrifugation at 12 000 rpm for 10 min. Then, 1.5 ml of 5% trichloroacetic acid containing 0.67% (w/v) thiobarbituric acid was added to 1.5 ml of the supernatant. The mixture was boiled for 30 min, quickly cooled on ice, and centrifuged at 12 000 *g* for 5 min. The absorbance of extracts was measured at A450, A532, and A600. The quantity of MDA was determined as C (μM/l) = 6.45 (A532 − A600) −0.56 × A450.

Measurement of Hydrogen Peroxide

The quantitative assay for H_2O_2 was performed essentially as described previously (Li et al., 2019) using the Amplex Red Hydrogen Peroxide assay kit (catalog no. A22188; Invitrogen). Briefly, about 100 mg of leaves was harvested and immediately frozen in liquid nitrogen. The frozen leaves were ground to fine powder and extracted with 1 ml of 1× reaction buffer (50 mM sodium phosphate [pH 7.4]), and 10 μl of the dissolved sample was diluted with 490 μl of 1× reaction buffer, of which 100 μl was used for the assay. Reaction mixtures (100 μl of the sample and 100 μl of Amplex red reagent/HRP working solution) were incubated in 96-well plates for 30 min at room temperature in the dark. A microplate reader (SpectraMax i3X) was used to detect the absorbance of H_2O_2 at 560 nm. The H_2O_2 concentration was calculated using a standard curve according to the manufacturer's protocol.

Measurement of Proline

Leaves (200 mg) were homogenized in 5 ml of 3% sulfosalicylic acid. The mixture was boiled for 10 min and then centrifuged at 3000 *g* for 20 min. Then, 1 ml of sample supernatant was mixed with 1 ml of acetic acid and 1 ml of ninhydrin reagent in a 10 ml tube and boiled for 30 min, then cooled on ice. An equal volume of toluene was added to each sample and samples were vibrated for 1 min, and then centrifuged at 1000 *g* for 5 min. The absorbance of the supernatant at A520 was measured using a spectrophotometer and then the contents of proline were calculated using a standard curve.

Measurement of Ascorbate Acid

Measurement of ascorbate acid was performed as previously described (Miyaji et al., 2015). About 100 mg of leaves was harvested and immediately frozen in liquid nitrogen. The frozen leaves were ground to a fine powder and extracted with 1 ml of 0.2 N HCl for 30 min at 4°C and then centrifuged at 16 000 *g* for 10 min at 4°C. Then, 0.5 ml of supernatant and AsA standards were neutralized with NaH_2PO_4 (pH 5.6) and NaOH as follows: first, 50 μl of 0.2 M NaH_2PO_4 (pH 5.6) was added, followed by 0.5 ml of 0.2 M NaOH. The pH was verified with pH indicator paper. The final pH of all samples was between 5 and 6. The neutralized supernatant was pretreated with 5 mM DTT for 30 min at room temperature. Next, 100 μl of supernatant or AsA standard (0, 0.25, 0.5, 0.75, 1.5 mM) was added to 250 μl of 0.2 M NaH_2PO_4 (pH 5.6) and 148 μl of double distilled water. Total ascorbate was determined by measuring the change in absorbance at 265 nm after the addition of 2 μl (0.5 units) of ascorbate oxidase (Sigma A0157) to the mixture. The contents of total ascorbate were calculated using a standard curve.

Measurement of Soluble Pi

The measurement of plant-soluble Pi was performed as previously described with minor modifications (Gu et al., 2017). Briefly, ∼0.2 g of fresh samples was homogenized in 1 ml of 10% (w/v) perchloric acid using an ice-cold mortar and pestle. The homogenate was then diluted 10-fold with 5% (w/v) perchloric acid and placed on ice for 30 min. After centrifugation at 12 000 *g* for 10 min at 4°C, the supernatant was used for Pi measurement using the molybdenum blue method: 4% (w/v) ammonium molybdate dissolved in 0.5 M H_2SO_4 (solution A) was mixed with 10% ascorbic acid (solution B) at a ratio of A:B = 6:1. A 2 ml aliquot of this working solution was added to 1 ml of the sample solution and incubated in a water bath at 42°C for 20 min. After cooling, the absorbance at 820 nm was measured by a spectrophotometer and then the contents of soluble Pi were calculated using a standard curve.

Measurement of ABA Content

Up to 100 mg of leaves was harvested, equally divided into two samples (samples 1 and 2) and the fresh weights were determined (FW1 and FW2). Next, sample 1 (∼50 mg) was dried at 65°C for 24 h and the dry mass was determined (DW1). Sample 2 was stored in liquid nitrogen immediately for ABA content measurement. Frozen leaves of sample 2 (∼50 mg) were ground to a fine power in liquid nitrogen in a 2ml tube using a pestle, and then mixed with 750 μl of cold extraction buffer 1 (methanol/water/acetic acid, 80:19:1, v/v/v, supplemented with 10 ng of ^{2H6}ABA as an internal standard), vigorously shaken on a shaking bed for 16 h at 4°C in the dark, and then centrifuged at 12 000 rpm for 15 min at 4°C. The supernatant was carefully transferred to a new 2 ml tube, and the pellet was resuspended with 400 μl of extraction buffer 2 (methanol/water/acetic acid, 80:19:1, v/v/v), shaken for 4 h at 4°C, then centrifuged. The two supernatants were combined and filtered using a syringe-facilitated 13 mm diameter nylon filter with a pore size of 0.22 μm. The filtrate was dried by evaporation under a flow of nitrogen gas for approximately 1 h at room

temperature, and then resuspended in 200 μl of methanol. ABA was quantified using an liquid chromatography-electrospray ionization-tandem mass spectrometry system as previously described (Liu et al., 2012). The ABA concentration of the samples (C, ng/ml) was calculated using an ABA standard curve (Sigma) ranging from 0 to 20 ng/ml. The ABA contents of the samples were determined as follows: C × 0.2/(DW1/FW1) × FW2.

Primers

All primers used in this study are listed in Supplemental Table 2.

SUPPLEMENTAL INFORMATION

Supplemental Information is available at *Molecular Plant Online*.

FUNDING

This work was supported by the National Key Research and Development Program of China (2016YFD0100600), the National Natural Science Foundation of China (31971954), the Thousand Talents Plan of China and the Fundamental Research Funds for the Central Universities of China (2662015PY170), and partly supported by the open funds of the National Key Laboratory of Crop Genetic Improvement.

AUTHOR CONTRIBUTIONS

M.D. conceived the project. H.Z., Y.X., N.H., H.L., and L.F. performed the experiments. X.S. and F.Z. carried out the bioinformatics analysis. D.Z. purified the proteins that were expressed in insect cells. X. Liu. managed the field growth of transgenic maize. M.D., H.Z., Y.X., and X. Li. designed the experiments and analyzed the data. M.D. and H.Z. wrote the manuscript. W.T. and J.Y. revised the article. All authors read and approved the final manuscript.

ACKNOWLEDGMENTS

We thank Dr. Ping Yin (Huazhong Agricultural University) for help in protein expression and purification from insect cells, and Dr. Haiyang Wang (Biotechnology Research Institute, Chinese Academy of Agricultural Sciences) for discussion. No conflict of interest declared.

Received: October 13, 2019
Revised: February 9, 2020
Accepted: February 10, 2020
Published: February 13, 2020

REFERENCES

Ahmed, F., Baloch, D.M., Hassan, M.J., and Ahmed, N. (2013). Role of plant growth regulators in improving oil quantity and quality of sunflower hybrids in drought stress. Biologia **59**:315–322.

Akram, N.A., Shafiq, F., and Ashraf, M. (2017). Ascorbic acid-A potential oxidant scavenger and its role in plant development and abiotic stress tolerance. Front. Plant Sci. **8**:613.

Amin, B., Mahleghah, G., Mahmood, H.M.R., and Hossein, M. (2009). Evaluation of interaction effect of drought stress with ascorbate and salicylic acid on some of physiological and biochemical parameters in okra (*Hibiscus esculentus* L.). Res. J. Biol. Sci. **4**:380–387.

Badejo, A.A., Fujikawa, Y., and Esaka, M. (2009). Gene expression of ascorbic acid biosynthesis related enzymes of the Smirnoff-Wheeler pathway in acerola (*Malpighia glabra*). J. Plant Physiol. **166**:652–660.

Barsotti, C., Pesi, R., Giannecchini, M., and Ipata, P.L. (2005). Evidence for the involvement of cytosolic 5′-nucleotidase (cN-II) in the synthesis of guanine nucleotides from xanthosine. J. Biol. Chem. **280**:13465–13469.

Bulley, S.M., Rassam, M., Hoser, D., Otto, W., Schünemann, N., Wright, M., MacRae, E., Gleave, A., and Laing, W. (2009). Gene expression studies in kiwifruit and gene over-expression in *Arabidopsis* indicates that GDP-L-galactose guanyltransferase is a major control point of vitamin C biosynthesis. J. Exp. Bot. **60**:765–778.

Choudhury, F.K., Rivero, R.M., Blumwald, E., and Mittler, R. (2017). Reactive oxygen species, abiotic stress and stress combination. Plant J. **90**:856–867.

Chu, H.M., Guo, R.T., Lin, T.W., Chou, C.C., Shr, H.L., Lai, H.L., Tang, T.Y., Cheng, K.J., Selinger, B.L., and Wang, A.H. (2004). Structures of *Selenomonas ruminantium* phytase in complex with persulfated phytate: DSP phytase fold and mechanism for sequential substrate hydrolysis. Structure **12**:2015–2024.

Conklin, P.L., Norris, S.R., Wheeler, G.L., Williams, E.H., Smirnoff, N., and Last, R.L. (1999). Genetic evidence for the role of GDP-mannose in plant ascorbic acid (vitamin C) biosynthesis. Proc. Natl. Acad. Sci. U S A **96**:4198–4203.

Conklin, P.L., Saracco, S.A., Norris, S.R., and Last, R.L. (2000). Identification of ascorbic acid-deficient *Arabidopsis thaliana* mutants. Genetics **154**:847–856.

Conklin, P.L., Gatzek, S., Wheeler, G.L., Dowdle, J., Raymond, M.J., Rolinski, S., Isupov, M., Littlechild, J.A., and Smirnoff, N. (2006). *Arabidopsis thaliana* VTC4 encodes L-galactose-1-P phosphatase, a plant ascorbic acid biosynthetic enzyme. J. Biol. Chem. **281**:15662–15670.

Dai, M., Zhang, C., Kania, U., Chen, F., Xue, Q., McCray, T., Li, G., Qin, G., Wakeley, M., Terzaghi, W., et al. (2012). A PP6-type phosphatase holoenzyme directly regulates PIN phosphorylation and auxin efflux in *Arabidopsis*. Plant Cell **24**:2497–2514.

Darvishan, M., Moghadam, H.R.T., and Nasri, M. (2013). Effect of foliar application of ascorbic acid (vitamin C) on yield and yield components of corn (*Zea mays* L.) as influenced by withholding of irrigation at different growth stages. Res. Crops **14**:736–742.

Ding, S., Zhang, B., and Qin, F. (2015). Arabidopsis RZFP34/CHYR1, a ubiquitin E3 ligase, regulates stomatal movement and drought tolerance via SnRK2.6-mediated phosphorylation. Plant Cell **27**:3228–3244.

Dowdle, J., Ishikawa, T., Gatzek, S., Rolinski, S., and Smirnoff, N. (2007). Two genes in *Arabidopsis thaliana* encoding GDP-L-galactose phosphorylase are required for ascorbate biosynthesis and seedling viability. Plant J. **52**:673–689.

Fujii, H., and Zhu, J.K. (2009). *Arabidopsis* mutant deficient in 3 abscisic acid-activated protein kinases reveals critical roles in growth, reproduction, and stress. Proc. Natl. Acad. Sci. U S A **106**:8380–8385.

Fujita, Y., Yoshida, T., and Yamaguchi-Shinozaki, K. (2013). Pivotal role of the AREB/ABF-SnRK2 pathway in ABRE-mediated transcription in response to osmotic stress in plants. Physiol. Plant **147**:15–27.

Gallie, D.R. (2013). The role of L-ascorbic acid recycling in responding to environmental stress and in promoting plant growth. J. Exp. Bot. **64**:433–443.

Gu, M., Zhang, J., Li, H., Meng, D., Li, R., Dai, X., and Wang, S. (2017). Maintenance of phosphate homeostasis and root development are coordinately regulated by MYB1, an R2R3-type MYB transcription factor in rice. J. Exp. Bot. **68**:3603–3615.

Guo, L., Chen, S., Liu, K., Liu, Y., Ni, L., Zhang, K., and Zhang, L. (2008). Isolation of heat shock factor HsfA1a-binding sites in vivo revealed variations of heat shock elements in *Arabidopsis thaliana*. Plant Cell Physiol. **49**:1306–1315.

He, Z., Zhong, J., Sun, X., Wang, B., Terzaghic, W., and Dai, M. (2018). The maize ABA receptors ZmPYL8, 9 and 12 facilitate plant drought resistance. Front. Plant Sci. **9**:422.

Hernández, J.A., Jiménez, A., Mullineaux, P., and Sevilla, F. (2000). Tolerance of pea (*Pisum sativum* L.) to long-term salt stress is associated with induction of antioxidant defences. Plant Cell Environ. **23**:853–862.

Himmelbach, A., Yang, Y., and Grill, E. (2003). Relay and control of abscisic acid signaling. Curr. Opin. Plant Biol. **6**:470–479.

Hussein, N.M., Hussein, M.I., Gadel Hak, S.H., and Hammad, M.A. (2014). Effect of two plant extracts and four aromatic oils on tuta absoluta population and productivity of tomato cultivar gold stone. Nat. Sci. **12**:108–118.

Hwang, S.M., Kim, D.W., Woo, M.S., Jeong, H.S., Son, Y.S., Akhter, S., Choi, G.J., and Bahk, J.D. (2014). Functional characterization of *Arabidopsis* HsfA6a as a heat-shock transcription factor under high salinity and dehydration conditions. Plant Cell Environ. **37**:1202–1222.

Ioannidi, E., Kalamaki, M.S., Engineer, C., Pateraki, I., Alexandrou, D., Mellidou, I., Giovannonni, J., and Kanellis, A.K. (2009). Expression profiling of ascorbic acid-related genes during tomato fruit development and ripening and in response to stress conditions. J. Exp. Bot. **60**:663–678.

Kaufmann, K., Muiño, J.M., Østerås, M., Farinelli, L., Krajewski, P., and Angenent, G.C. (2010). Chromatin immunoprecipitation (ChIP) of plant transcription factors followed by sequencing (ChIP-SEQ) or hybridization to whole genome arrays (ChIP-CHIP). Nat. Protoc. **5**:457–472.

von Koskull-Döring, P., Scharf, K.D., and Nover, L. (2007). The diversity of plant heat stress transcription factors. Trends Plant Sci. **12**:452–457.

Kuznetsova, E., Proudfoot, M., Sanders, S.A., Reinking, J., Savchenko, A., Arrowsmith, C.H., Edwards, A.M., and Yakunin, A.F. (2005). Enzyme genomics: application of general enzymatic screens to discover new enzymes. FEMS Microbiol. Rev. **29**:263–279.

Leung, J., and Giraudat, J. (1998). Abscisic acid signal transduction. Annu. Rev. Plant Physiol. Plant Mol. Biol. **49**:199–222.

Li, Y., Cao, X.L., Zhu, Y., Yang, X.M., Zhang, K.N., Xiao, Z.Y., Wang, H., Zhao, J.H., Zhang, L.L., Li, G.B., et al. (2019). Osa-miR398b boosts H_2O_2 production and rice blast disease-resistance via multiple superoxide dismutases. New Phytol. **222**:1507–1522.

Linster, C.L., Gomez, T.A., Christensen, K.C., Adler, L.N., Young, B.D., Brenner, C., and Clarke, S.G. (2007). Arabidopsis VTC2 encodes a GDP-L-galactose phosphorylase,the last unknown enzyme in the Smirnoff-Wheeler pathway to ascorbic acid in plants. J. Biol. Chem. **282**:18879–18885.

Liu, H., Li, X., Xiao, J., and Wang, S. (2012). A convenient method for simultaneous quantification of multiple phytohormones and metabolites: application in study of rice-bacterium interaction. Plant Methods **8**:2.

Ma, Y., Szostkiewicz, I., Korte, A., Moes, D., Yang, Y., Christmann, A., and Grill, E. (2009). Regulators of PP2C phosphatase activity function as abscisic acid sensors. Science **324**:1064–1068.

Ma, L., Wang, Y., Liu, W., and Liu, Z. (2014). Overexpression of an alfalfa GDP-mannose 3, 5-epimerase gene enhances acid, drought and salt tolerance in transgenic *Arabidopsis* by increasing ascorbate accumulation. Biotechnol. Lett. **36**:2331–2341.

Malik, S., and Ashraf, M. (2012). Exogenous application of ascorbic acid stimulates growth and photosynthesis of wheat (*Triticum aestivum* L.) under drought. Soil Environ. **31**:72–77.

Mancinelli, A.L. (1990). Interaction between light quality and light quantity in the photoregulation of anthocyanin production. Plant Physiol. **92**:1191–1195.

Mittler, R. (2017). ROS are good. Trends Plant Sci. **22**:11–19.

Miyaji, T., Kuromori, T., Takeuchi, Y., Yamaji, N., Yokosho, K., Shimazawa, A., Sugimoto, E., Omote, H., Ma, J.F., Shinozaki, K., et al. (2015). AtPHT4 is a chloroplast-localized ascorbate transporter in *Arabidopsis*. Nat. Commun. **6**:5928.

Nover, L., Bharti, K., Döring, P., Mishra, S.K., Ganguli, A., and Scharf, K.D. (2001). *Arabidopsis* and the heat stress transcription factor world, how many heat stress transcription factors do we need? Cell Stress Chaperones **6**:177–189.

Ohama, N., Sato, H., Shinozaki, K., and Yamaguchi-Shinozaki, K. (2017). Transcriptional regulatory network of plant heat stress response. Trends Plant Sci. **22**:53–65.

Ou, B., Yin, K.Q., Liu, S.N., Yang, Y., Gu, T., Wing Hui, J.M., Zhang, L., Miao, J., Kondou, Y., Matsui, M., et al. (2011). A high-throughput screening system for *Arabidopsis* transcription factors and its application to Med25-dependent transcriptional regulation. Mol. Plant **4**:546–555.

Park, S.Y., Szostkiewicz, I., Korte, A., Moes, D., Yang, Y., Christmann, A., and Grill, E. (2009). Abscisic acid inhibits type 2C protein phosphatases via the PYR/PYL family of START proteins. Science **324**:1068–1071.

Pastori, G.M., and Foyer, C.H. (2002). Common components, networks, and pathways of cross-tolerance to stress. The central role of "redox" and abscisic acid-mediated controls. Plant Physiol. **129**:460–468.

Quintero, F.J., Garciadeblás, B., and Rodríguez-Navarro, A. (1996). The SAL1 gene of *Arabidopsis*, encoding an enzyme with 3'(2'),5'-bisphosphate nucleotidase and inositol polyphosphate 1-phosphatase activities, increases salt tolerance in yeast. Plant Cell **8**:529–537.

Raghavendra, A.S., Gonugunta, V.K., Christmann, A., and Grill, E. (2010). ABA perception and signalling. Trends Plant Sci. **15**:395–401.

Rodríguez, V.M., Chételat, A., Majcherczyk, P., and Farmer, E.E. (2010). Chloroplastic phosphoadenosine phosphosulfate metabolism regulates basal levels of the prohormone jasmonic acid in *Arabidopsis* leaves. Plant Physiol. **152**:1335–1345.

Shafiq, S., Akram, N.A., Ashraf, M., and Arshad, A. (2014). Synergistic effects of drought and ascorbic acid on growth, mineral nutrients and oxidative defense system in canola (*Brassica napus* L.) plants. Acta Physiol. Plant **36**:1539–1553.

Shalata, A., Mittova, V., Volokita, M., Guy, M., and Tal, M. (2001). Response of the cultivated tomato and its wild salt-tolerant relative *Lycopersicon pennellii* to salt-dependent oxidative stress: the root antioxidative system. Physiol. Plant **112**:487–494.

Smirnoff, N., and Pallanca, J.E. (1996). Ascorbate metabolism in relation to oxidative stress. Biochem. Soc. Trans. **24**:472–478.

Urzica, E.I., Adler, L.N., Page, M.D., Linster, C.L., Arbing, M.A., Casero, D., Pellegrini, M., Merchant, S.S., and Clarke, S.G. (2012). Impact of oxidative stress on ascorbate biosynthesis in *Chlamydomonas* via regulation of the VTC2 gene encoding a GDP-L-galactose phosphorylase. J. Biol. Chem. **287**:14234–14245.

Valpuesta, V., and Botella, M.A. (2004). Biosynthesis of L-ascorbic acid in plants, new pathways for an old antioxidant. Trends Plant Sci. **9**:573–577.

Wang, Y., Cai, S., Yin, L., Shi, K., Xia, X., Zhou, Y., Yu, J., and Zhou, J. (2015). Tomato HsfA1a plays a critical role in plant drought tolerance by activating ATG genes and inducing autophagy. Autophagy **11**:2033–2047.

Wang, X., Feng, J., Xue, Y., Guan, Z., Zhang, D., Liu, Z., Gong, Z., Wang, Q., Huang, J., Tang, C., et al. (2016). Structural basis of N(6)-adenosine methylation by the METTL3-METTL14 complex. Nature **534**:575–578.

Wheeler, G.L., Jones, M.A., and Smirnoff, N. (1998). The biosynthetic pathway of vitamin C in higher plants. Nature **393**:365–369.

Wilson, P.B., Estavillo, G.M., Field, K.J., Pornsiriwong, W., Carroll, A.J., Howell, K.A., Woo, N.S., Lake, J.A., Smith, S.M., Harvey Millar, A., et al. (2009). The nucleotidase/phosphatase SAL1 is a negative regulator of drought tolerance in *Arabidopsis*. Plant J. **58**:299–317.

Xiang, Y., Sun, X., Gao, S., Qin, F., and Dai, M. (2017). Deletion of an endoplasmic reticulum stress response element in a ZmPP2C-A

gene facilitates drought tolerance of maize seedlings. Mol. Plant **10**:456–469.

Xiong, L., Lee, H., Huang, R., and Zhu, J.K. (2004). A single amino acid substitution in the *Arabidopsis* FIERY1/HOS2 protein confers cold signaling specificity and lithium tolerance. Plant J. **40**:536–545.

Yazdanpanah, S., Baghizadeh, A., and Abbassi, F. (2011). The interaction between drought stress and salicylic and ascorbic acids on some biochemical characteristics of *Satureja hortensis*. Afric. J. Agric. Res. **6**:798–807.

Yoshiba, Y., Kiyosue, T., Nakashima, K., Yamaguchi-Shinozaki, K., and Shinozaki, K. (1997). Regulation of levels of proline as an osmolyte in plants under water stress. Plant Cell Physiol. **38**:1095–1102.

Yoshida, T., Fujita, Y., Sayama, H., Kidokoro, S., Maruyama, K., Mizoi, J., Shinozaki, K., and Yamaguchi-Shinozaki, K. (2010). AREB1, AREB2, and ABF3 are master transcription factors that cooperatively regulate ABRE-dependent ABA signaling involved in drought stress tolerance and require ABA for full activation. Plant J. **61**:672–685.

Yoshimura, K., Nakane, T., Kume, S., Shiomi, Y., Maruta, T., Ishikawa, T., and Shigeoka, S. (2014). Transient expression analysis revealed the importance of VTC2 expression level in light/dark regulation of ascorbate biosynthesis in *Arabidopsis*. Biosci. Biotechnol. Biochem. **78**:60–66.

Yu, H., Zhang, Y., Xie, Y., Wang, Y., Duan, L., Zhang, M., and Li, Z. (2017). Ethephon improved drought tolerance in maize seedlings by modulating cuticular wax biosynthesis and membrane stability. J. Plant Physiol. **214**:123–133.

Zhao, Y., Chan, Z., Gao, J., Xing, L., Cao, M., Yu, C., Hu, Y., You, J., Shi, H., Zhu, Y., et al. (2016). ABA receptor PYL9 promotes drought resistance and leaf senescence. Proc. Natl. Acad. Sci. U S A **113**:1949–1954.